

Multiple ALPs and enhanced echoes

Shihabul Haque^a and Sourov Roy^a

^a*School of Physical Sciences, Indian Association for the Cultivation of Science, 2A and 2B Raja S.C. Mullick Road, Kolkata 700032, India*

E-mail: shihabul1312@gmail.com, tps@iacs.res.in

ABSTRACT: We present a theoretical study of axion echoes in the context of multiple ALP models. We begin by reviewing the single ALP case, deriving the conditions for resonance and echo formation. Starting from a set of N ALPs coupling to the photon, we then derive the relevant echo equations for both coherent and incoherent configurations. In the former case, we show that the echo power scales with N leading to sharper amplification and potentially improving projected bounds discussed earlier in literature. Small mass splittings between the ALPs further increase this amplification, even for a $N = 2$ case. We also outline the potential experimental implications of our results and discuss prospects for detecting these echoes in a wide range of ALP masses. In the incoherent scenario, we show that the random phases lead to a suppression of the echo power, eventually resulting in observable signals akin to or even weaker than the single ALP case.

KEYWORDS: Axion, axion echoes, ALP/photon interaction, multiple ALPs

Contents

1	Introduction	1
2	Perturbative approach for single ALP	3
2.1	Perturbative solution	4
2.2	Power carried by the echo wave	5
3	The multiple ALP scenario	7
3.1	Coherent scenario for general distributions	8
3.2	All masses and couplings equal	10
3.3	Variable couplings and all masses equal	11
3.4	Variable masses and all couplings equal	13
4	The incoherent scenario	15
4.1	Incoherent scenario for general distributions	16
4.2	All masses equal	18
4.3	Variable couplings and all masses equal	19
5	Discussions	20
A	Standard solution of a forced oscillator	21
B	Validity of large N approximation	22
C	Solution of the multi-ALP echo system	25
C.1	General solution	25
C.2	Resonant response	27
C.3	Real space solution	29
C.4	Power calculation	29

1 Introduction

In recent years, the axion has become a point of major interest for beyond-standard-model physics. First proposed as a solution to the Strong CP problem in particle physics through the Peccei-Quinn mechanism [1–3], the QCD axion [4–7] grew to encompass another potential role, namely as a dark matter (DM) candidate [8–11]. It was also realised that in several beyond-standard-model contexts, light or ultralight pseudoscalar particles often arise naturally and could fulfill the same role as a potential DM candidate. These were dubbed axion-like particles (ALPs). Altogether, the field of axion (or, ALP) physics is rich and dynamic, both from a theory perspective as well as a phenomenology perspective.

For a detailed description of the current status of the ALP in various contexts, see, for example, [12–17].

In the context of ALP phenomenology, a recent area of much interest has been the idea of axion echoes. The most general form of the ALP/photon interaction Lagrangian for a set of N ALPs is given by,

$$\mathcal{L}_{int} = -\frac{1}{4} \sum_{i=1}^N g_{a\gamma\gamma}^i a^i F_{\mu\nu} \tilde{F}^{\mu\nu} \quad (1.1)$$

The form of the above interaction implies two simple processes by which ALPs can interact with photons - one is the standard ALP/photon oscillation wherein the ALP and photon modes mix with each other in the presence of an external electromagnetic field [18]. A second process involves the straightforward decay of an ALP into two photons. With regards to this latter situation, it can be shown that the decay rates are amplified in the presence of an external electromagnetic field, i.e., an incident photon, with momentum equal to half the mass of the ALP [19]. Because of the conservation of momentum, one of the newly generated photons is emitted in the direction of the initial incident photon while the other has a momentum opposite to it. Since the latter photon travels opposite to the incident wave, it is termed an “echo” wave and this entire phenomenon is called an “axion echo”. The feasibility of detecting such echo waves has been extensively studied in recent literature. In [20–22], the idea of sending out a beam into space and looking for the resulting echo waves, for example by using the 21 CentiMeter Array (21CMA) [23] or the Square Kilometer Array (SKA) [24], has been discussed in much detail. Other studies have focused on echoes generated by photon flux from distinct astrophysical sources. References [25, 26] discuss the possibility of looking at echoes induced by supernovae remnants which would have had a significant photon flux in the past while [27] considers the flux from Cygnus A, one of the strongest radio sources in the sky. Reference [28] discusses axion echoes generated by spheroidal galaxies while reference [29] discusses axion echoes in detail, specifically focusing on galactic pulsars.

ALPs also arise naturally in several string theory contexts and warped geometry models, several of which often suggest not one but a set of multiple ALPs [30–32]. Such multiple ALPs can also arise from a clockwork mechanism [33–36]. Recently, reference [37] considered a general ALP anarchy case and reinterpreted previous ALP signals in different experimental contexts. Specifically, they showed that the multiple ALP phenomenology could be drastically different from the single ALP case, for example, leading to a weaker signal in experiments such as CAST [38]. Similarly, recent references like [39] and [40] also show how the multi-axion situation is distinct from the single ALP scenario and presents novel and interesting results. In such a situation, we believe it is worthwhile to explore how the phenomenology of axion echoes might change for multiple ALPs and how it can affect future search prospects.

In this work, we start from a minimal model and present a theoretical study of axion echoes in the context of multiple ALPs. In section 2, we briefly derive the relevant equations and projected bounds following reference [20] in the single ALP case. We extend our arguments in section 3 to the multiple ALP case. We consider the simplest possible multiple ALP model with a set of N ALPs, all coupling to the Standard Model (SM) photon, with the masses and coupling strengths distributed in a certain range, according to some distribution functions. We consider two broad scenarios, coherent, with the ALP fields oscillating in phase, and incoherent, when the phases are assumed to be random, and derive the relevant equation in details. For the coherent case, we show that the echo power scales as N , leading to an amplification depending on the number of ALPs in the theory. We also consider the case of ALPs with small mass splittings as might happen naturally in various string based models or in models with ALPs featuring a clockwork mechanism for mass generation and show that the mass splitting parameter causes additional amplification leading to improvements in projected bounds even for a minimal $N = 2$ case. In section 4, we present a similar treatment of the incoherent setup and show that the earlier amplification is lost - in fact, the projected constraints can be shown to be weaker than even the single ALP scenario. Echo calculations are dependent on the exact DM density profile chosen; here, we mostly follow the standard isothermal profile [41] used commonly in axion echo literature in order to facilitate the easy and convenient comparison of results in the two cases. Our calculations and arguments can be extended to other DM density profiles when required. We present a discussion of our results in section 5. Detailed calculations are presented in the appendices.

2 Perturbative approach for single ALP

In this section, we will briefly review the derivation of the echo wave in the case of a single ALP in the spirit of reference [20] in order to set the stage for the more complicated case of multiple ALPs. The basic idea is as follows - we send out a beam of photons from the earth in the direction of the ALP DM distribution, aiming to capture the resultant echo photons that return back to earth following the decay of the ALP DM into photons as described earlier. We begin with the usual interaction Lagrangian,

$$\mathcal{L}_{int} = -\frac{1}{4}g_{a\gamma\gamma}aF_{\mu\nu}\tilde{F}^{\mu\nu} \quad (2.1)$$

Our ALP field is denoted by $a(x)$ while the photons are described by $F^{\mu\nu}$. The Maxwell equations in presence of such an interaction term are given by,

$$\partial_\mu F^{\mu\nu} = g_{a\gamma\gamma}\partial_\mu a\tilde{F}^{\mu\nu} \quad (2.2)$$

Since we are considering plane waves, we have, in the Coulomb gauge,

$$A^0 = 0, \quad \nabla \cdot \vec{A} = 0 \quad (2.3)$$

The ALP dark matter (DM) is usually assumed to be non-relativistic leading to a negligible gradient. This allows us to write,

$$\square \vec{A}(t, \vec{x}) = -g_{a\gamma\gamma}\partial_t a(\nabla \times \vec{A}(t, \vec{x})) \quad (2.4)$$

The ALP DM, assumed to be static, can be written down as,

$$a(t, \vec{x}) = \mathcal{A}_0 \sin(m_a t) \quad (2.5)$$

This is derived from the equations of motion for the ALP field (ignoring backreaction). Here, \mathcal{A}_0 represents the amplitude factor, which is related to the DM density as,

$$\rho = \frac{1}{2} m_a^2 \mathcal{A}_0^2 \quad (2.6)$$

Here, ρ is the DM density while m_a is the mass of the ALP. Using eqs. (2.4) and (2.5), we get,

$$\square \vec{A}(t, \vec{x}) = -g \cos(m_a t) (\nabla \times \vec{A}(t, \vec{x})) \quad (2.7)$$

Where, $g = g_{a\gamma\gamma} m_a \mathcal{A}_0$. In Fourier space, our equation becomes,

$$(\partial_t^2 + p^2) \vec{A}_p(t, \vec{p}) = -ig \cos(m_a t) [\vec{p} \times \vec{A}_p(t, \vec{p})] \quad (2.8)$$

This is what we shall be working with.

2.1 Perturbative solution

We assume that the photon field can be written as,

$$\vec{A}_p = \vec{A}_0^p + \vec{A}_1^p \quad (2.9)$$

Here, \vec{A}_0^p is the initial incident radiation while \vec{A}_1^p is the smaller correction generated by the interaction term with the ALP. Assuming that g is small, we have, in the zeroth order,

$$(\partial_t^2 + p^2) \vec{A}_0^p = 0 \Rightarrow \vec{A}_0^p = \vec{A} e^{-ipt} + \vec{B} e^{ipt} \quad (2.10)$$

Note that we use $p^\mu = (p, \vec{p})$ to denote the 4-momentum of the photon since $p^\mu p_\mu = 0$. Since we start with an outgoing beam of radiation, we must have,

$$\vec{A}_0(t, \vec{x}) = \vec{a}_0 e^{i(\vec{k} \cdot \vec{x} - kt)}, \quad \dot{\vec{A}}_0(t, \vec{x}) = -ik \vec{a}_0 e^{i(\vec{k} \cdot \vec{x} - kt)} \quad (2.11)$$

This implies,

$$\vec{A} = \frac{1}{2} \vec{a}_0 \delta^{(3)}(\vec{k} - \vec{p}) \left[1 + \frac{k}{p} \right], \quad \vec{B} = \frac{1}{2} \vec{a}_0 \delta^{(3)}(\vec{k} - \vec{p}) \left[1 - \frac{k}{p} \right] \quad (2.12)$$

Thus,

$$\vec{A}_0^p = \vec{a}_0 \delta^{(3)}(\vec{k} - \vec{p}) \left[\cos(pt) - i \frac{k}{p} \sin(pt) \right] = \vec{a}_0 \delta^{(3)}(\vec{k} - \vec{p}) e^{-ipt} \quad (2.13)$$

The last equality is imposed by the delta function and the fact that the photon four-momentum has null norm. Now, in first order, we have,

$$(\partial_t^2 + p^2) \vec{A}_1^p = -ig \cos(m_a t) [\vec{p} \times \vec{A}_0^p] = -\frac{ig}{2} \delta^{(3)}(\vec{k} - \vec{p}) (\vec{p} \times \vec{a}_0) \left(e^{i(m_a - p)t} + e^{-i(m_a + p)t} \right) \quad (2.14)$$

Let us define,

$$\vec{B}_{kp} = \frac{g}{2} (\vec{p} \times \vec{a}_0) \delta^{(3)}(\vec{k} - \vec{p}) \quad (2.15)$$

Then,

$$(\partial_t^2 + p^2)\vec{A}_1^p = -i\vec{B}_{kp}\left(e^{i(m_a-p)t} + e^{-i(m_a+p)t}\right) \quad (2.16)$$

This is the equation of a simple forced oscillator. The solution to such an equation can be written as (see appendix A),

$$\vec{A}_1^p = \frac{i}{m_a}\vec{B}_{kp}\left[\frac{e^{i(m_a-p)t}}{m_a-2p} + \frac{e^{-i(m_a+p)t}}{m_a+2p} - \frac{2m_a e^{ipt}}{(m_a-2p)(m_a+2p)}\right] \quad (2.17)$$

It can be seen clearly from the above equation that resonance occurs if $p = m_a/2$, i.e., the photon momentum has to be half the axion mass. Let us consider the situation at resonance. We then have $p = m_a/2 + \delta$ where δ is very small. We consider only the dominant terms,

$$\vec{A}_1^p \approx -\frac{i}{m_a}\vec{B}_{kp}\left[\frac{e^{i(p-2\delta)t}}{2\delta} - \frac{e^{ipt}}{2\delta}\right] = \frac{i}{4p\delta}\vec{B}_{kp}e^{ipt}\left(1 - e^{-2i\delta t}\right) \quad (2.18)$$

We expand the exponential and take the $\delta \rightarrow 0$ limit which gives us,

$$\vec{A}_1^p \approx -\frac{t}{2p}\vec{B}_{kp}e^{ipt} \quad (2.19)$$

Performing an inverse Fourier transform to go back to real space, we have,

$$\vec{A}_1(t, \vec{x}) = -\int \frac{d^3p}{(2\pi)^3} \frac{t}{2p} e^{ipt} \left(\frac{g}{2}(\vec{p} \times \vec{a}_0)\delta^{(3)}(\vec{k} - \vec{p})\right) e^{i\vec{p}\cdot\vec{x}} = -\frac{g}{4}t(\hat{k} \times \vec{a}_0)e^{i(\vec{k}\cdot\vec{x}+kt)} \quad (2.20)$$

The total solution (up to first order) is then,

$$\vec{A}(t, \vec{x}) = \vec{a}_0 e^{i(\vec{k}\cdot\vec{x}-kt)} - \frac{g}{4}t(\hat{k} \times \vec{a}_0)e^{i(\vec{k}\cdot\vec{x}+kt)} \quad (2.21)$$

The second term arising from the interaction has two distinct features - one, its polarisation is orthogonal to that of the outgoing beam, and, second, it travels in the opposite direction to the outgoing wave. This is the *echo wave*.

2.2 Power carried by the echo wave

We now present a brief derivation of the power carried by the echo wave. We start from eq. (2.18),

$$\vec{A}_1^p = \frac{i}{4p\delta}\vec{B}_{kp}e^{ipt}(1 - e^{-2i\delta t}) = -\frac{1}{2p}\vec{B}_{kp}e^{ipt}\frac{\sin(\delta t)}{\delta}e^{-i\delta t} \quad (2.22)$$

The power is defined as,

$$P = \int dp |\vec{A}(t, \vec{p})|^2 = \int dp \frac{1}{4p^2} |\vec{B}_{kp}|^2 \left(\frac{\sin(\delta t)}{\delta}\right)^2 \quad (2.23)$$

For long times, we have,

$$\left(\frac{\sin(\delta t)}{\delta}\right)^2 \rightarrow \pi t \delta(\delta) \quad (2.24)$$

Thus, for the echo wave,

$$P = \left[\frac{\pi g^2 t}{16} \frac{dP_0}{dp} \right]_{p=m_a/2} \quad (2.25)$$

Where,

$$\frac{dP_0}{dp} = |\vec{A}_0^p(t, \vec{p})|^2 = a_0^2 \delta^{(3)}(\vec{k} - \vec{p}) \quad (2.26)$$

Using $g^2 = (g_{a\gamma\gamma} m_a \mathcal{A}_0)^2 = 2g_{a\gamma\gamma}^2 \rho$ and expressing $\omega/2\pi = \nu$, we finally arrive at,

$$P = g_{a\gamma\gamma}^2 \frac{t}{16} \rho \frac{dP_0}{d\nu} \Big|_{k=m_a/2} \quad (2.27)$$

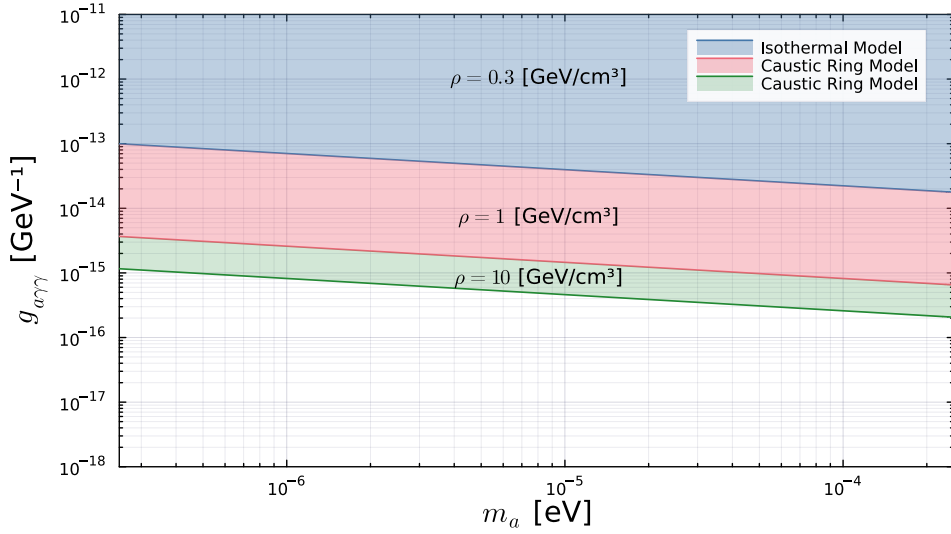


Figure 1. Constraining the parameter space with axion echoes with an outgoing energy of 10 MW per year per factor of two in ALP mass.

The projected bounds obtained thus are shown in figure 1 for two starkly different DM density profiles, the caustic ring profile and the isothermal profile. The isothermal model usually proposes a local DM density of around $0.3 \text{ [GeV/cm}^3\text{]}$ while in the caustic ring model, this value is generally higher because of the earth's proximity to a caustic ring in the Milky Way galaxy [42, 43] leading to much stronger bounds. As mentioned earlier, the nature of the bounds depends on the DM density profile under consideration. For the sake of easy comparison between different cases, we henceforth follow the standard isothermal model as outlined in reference [20]. For rough experimental estimates, we replace t in eq. (2.27) with CR/v_\perp where R is the detector radius, v_\perp is the magnitude of the velocity of the ALP DM perpendicular to the outgoing photon wave and C is an order one number that captures the effect of the configuration of the detector with respect to the DM distribution. While our calculations here apply to the situation where both the source of photons and the ALP DM are at rest, the conclusions are not altered significantly if we assume that the ALP DM has a small velocity with respect to the source in some direction. This is

the more realistic case and due to the ALP DM velocity, the echo wave is displaced in a transverse direction by an amount depending directly on the transverse velocity of the ALP DM - in other words, the echo wave returns to a point slightly displaced from its point of emission and this displacement is directly dependent on the transverse velocity of the ALP DM. The maximum possible displacement that the echo wave can undergo while still being detectable is simply R , the radius of the detector, and the time corresponding to this extremal scenario is R/v_\perp . Therefore, this substitution effectively captures the maximum displacement the echo can undergo while still being in the range of our detector and corresponds to the time it takes for the echo wave to travel the distance between our detector and the ALP distribution. Since, our main purpose in this work is to highlight the difference between the multi-ALP and single ALP scenarios, we use the same parameter values for both the DM distribution and the detector as in [20] unless mentioned otherwise (we refer those interested to eq. (12) and the discussion following it in the above reference).

3 The multiple ALP scenario

We consider a situation where we have a set of N ALPs in our theory. In principle, these ALPs can interact with both fermionic and vector fields, but we only focus on their coupling with photons. In general, we do not expect the mass matrix of these ALPs to be diagonal and there will be intermixing; however, in our case, this does not matter because we only consider couplings to the photon field. To make this clearer, let us consider the most general case with an off-diagonal mass matrix,

$$\mathcal{L}_{alp} = \frac{1}{2} \sum_{n,m=1}^N [\delta^{mn} \partial^\mu a_m \partial_\mu a_n - (m_a^{mn})^2 a_m a_n] - \frac{1}{4} \sum_{n=1}^m g_{a\gamma\gamma}^n a_n F_{\mu\nu} \tilde{F}^{\mu\nu} \quad (3.1)$$

In the above, only the first m ALPs couple to the standard model photon; the rest do not and are “hidden”. We now consider a transformation that takes us to the physical basis where the mass matrix is completely diagonal,

$$\begin{aligned} a_n = U_{nk} \tilde{a}_k &\Rightarrow \mathcal{L}_{alp} = \frac{1}{2} \sum_{n=1}^N [\partial^\mu \tilde{a}_n \partial_\mu \tilde{a}_n - (m_a^n)^2 \tilde{a}_n^2] - \frac{1}{4} \sum_{n=1}^m \left(\sum_{k=1}^N U_{nk} g_{a\gamma\gamma}^n \right) \tilde{a}_k F_{\mu\nu} \tilde{F}^{\mu\nu} \\ &\Rightarrow \mathcal{L}_{alp} = \frac{1}{2} \sum_{k=1}^N [\partial^\mu \tilde{a}_k \partial_\mu \tilde{a}_k - (m_a^k)^2 \tilde{a}_k^2] - \frac{1}{4} \sum_{k=1}^m \tilde{g}_{a\gamma\gamma}^k \tilde{a}_k F_{\mu\nu} \tilde{F}^{\mu\nu} \end{aligned} \quad (3.2)$$

Since the original mass matrix is real and symmetric, the transformation has to be orthogonal. As we cannot differentiate between the initial and final coupling strengths ($g_{a\gamma\gamma}^n$ and $\tilde{g}_{a\gamma\gamma}^n$) experimentally, it does not matter whether the mass matrix is diagonal or whether it needs to be diagonalised first. We can also see that the “hidden” ALPs also couple to the SM photon as part of the transformed field. Therefore, we only work with a situation where all the ALPs are diagonal and are coupled to the SM photon. Following the steps outlined in section 2, we find the following equation in the momentum space for the correction term,

$$(\partial_t^2 + p^2) \vec{A}_1^p = -i \sum_{n=1}^N \vec{B}_{kp}^n \left[e^{i(m_a^n - p)t} + e^{-i(m_a^n + p)t} \right] \quad (3.3)$$

With,

$$\vec{B}_{kp}^n = \frac{g_n}{2}(\vec{p} \times \vec{a}_0)\delta^{(3)}(\vec{k} - \vec{p}), \quad g_n = g_{a\gamma\gamma}^n m_a^n \mathcal{A}_0 \quad (3.4)$$

In general, the solution will be a superposition of all the different oscillations,

$$\vec{A}_1^p = \sum_{n=1}^N \frac{i}{m_a^n} \vec{B}_{kp}^n \left[\frac{e^{i(m_a^n - p)t}}{m_a^n - 2p} + \frac{e^{-i(m_a^n + p)t}}{m_a^n + 2p} - \frac{2m_a^n e^{ipt}}{(m_a^n - 2p)(m_a^n + 2p)} \right] \quad (3.5)$$

In this case, we have N separate resonance conditions - the solution will grow whenever $p = m_a^n/2$ for any $n \in [1, N]$. If all of the masses and couplings are distinct, then, only one resonance condition can be satisfied at any given time. Suppose we choose $p = m_a^j/2 = p_j$ for any j in the relevant range - this means the j -th term in the above solution will dominate over the rest. Therefore, we will have,

$$\vec{A}_1^p \approx -\frac{t}{2p_j} \vec{B}_{kp}^j e^{ip_j t} \quad (3.6)$$

The real space solution will take the form,

$$\vec{A}(t, \vec{x}) = \vec{a}_0 e^{i(\vec{k}_j \cdot \vec{x} - k_j t)} - \frac{g_j}{4} t (\hat{k}_j \times \vec{a}_0) e^{i(\vec{k}_j \cdot \vec{x} + k_j t)} \quad (3.7)$$

Observationally, this is similar to the case of only one ALP. These conclusions would apply to physically relevant examples such as Kaluza-Klein towers of ALPs where the fields all have distinct masses (and, therefore, distinct frequencies and resonance conditions) [44]. In fact, this could be an interesting way to probe the phenomenology of such theories. However, here, we consider two separate kinds of scenarios - a coherent case and an incoherent case - and specifically focus on the situation where there is not much hierarchy in the ALP masses (i.e., the difference between the most massive ALP and the least massive ALP is small). In general, the ALP fields can be expressed as,

$$a_n(t, \vec{x}) = \mathcal{A}_0 \sin(m_a^n t + \theta_n), \quad n \in [1, N] \quad (3.8)$$

Here, θ_n is a random phase factor. In the following section, we consider a case where all ALPs have the same phase (which we set to zero for simplicity). This might occur if all the ALPs have the same production mechanism, for instance, and are produced in the same region of space and time. This is what we call a ‘‘coherent’’ scenario. In section 4, we will consider the incoherent case by explicitly taking into account the random phases.

3.1 Coherent scenario for general distributions

The most general equation we can write down is,

$$(\partial_t^2 + p^2) \vec{A}_1^p = -i \mathcal{A}_0 (\vec{p} \times \vec{a}_0) \delta^{(3)}(\vec{p} - \vec{k}) e^{-ipt} \sum_{n=1}^N g_{a\gamma\gamma}^n m_a^n \cos(m_a^n t) \quad (3.9)$$

Let us now assume that we have N ALPs with distinct masses and couplings all distributed according to some distribution functions, $p(m_a)$ and $\tilde{p}(g_{a\gamma\gamma})$, respectively. We assume that each of the ALP masses and coupling strengths are distributed according to these

function in the intervals $[m_a^L, m_a^M]$ and $[g_{a\gamma\gamma}^L, g_{a\gamma\gamma}^M]$, respectively. Further, we assume that the distribution functions are normalized and independent of each other, i.e., the joint probability distribution is separable,

$$P_{\text{joint}}(m_a, g_{a\gamma\gamma}) = p(m_a)\tilde{p}(g_{a\gamma\gamma}) \quad (3.10)$$

With these assumptions, our masses and coupling strengths become akin to two independent sets of identically distributed random variables. As described in appendix B, in the large N limit, by the Law of Large Numbers, this goes to,

$$(\partial_t^2 + p^2)\vec{A}_1^p = -iN\mathcal{A}_0(\vec{p} \times \vec{a}_0)\delta^{(3)}(\vec{p} - \vec{k})e^{-ipt} \int_{g_{a\gamma\gamma}^L}^{g_{a\gamma\gamma}^M} g_{a\gamma\gamma}\tilde{p}(g_{a\gamma\gamma}) dg_{a\gamma\gamma} \int_{m_a^L}^{m_a^M} m_a \cos(m_a t) p(m_a) dm_a \quad (3.11)$$

Note that the coupling distribution, $\tilde{p}(g_{a\gamma\gamma})$, does not affect the dynamics of the system. Only the mass distribution does. Therefore, let us write this as,

$$(\partial_t^2 + p^2)\vec{A}_1^p = -2iN\vec{D}_{kp}e^{-ipt}Q(t) \quad (3.12)$$

Here,

$$\vec{D}_{kp} = \frac{1}{2}\mathcal{A}_0(\vec{p} \times \vec{a}_0)\delta^{(3)}(\vec{p} - \vec{k}) \int_{g_{a\gamma\gamma}^L}^{g_{a\gamma\gamma}^M} g_{a\gamma\gamma}\tilde{p}(g_{a\gamma\gamma}) dg_{a\gamma\gamma} \quad (3.13)$$

And,

$$Q(t) = \int_{m_a^L}^{m_a^M} m_a \cos(m_a t) p(m_a) dm_a \quad (3.14)$$

In order to proceed further, we assume that the mass splitting, defined as $\epsilon = (m_a^M - m_a^L)/2$, is small (i.e., $\epsilon \ll m_a^L$). In this case, as derived in appendix C, the final real space solution can be shown to be,

$$\vec{A}(t, \vec{x}) = \vec{a}_0 e^{i(\vec{k} \cdot \vec{x} - kt)} - N \frac{\tilde{g}t}{2} (\hat{k} \times \vec{a}_0) \left[a_1 + \frac{i}{2} a_2 \epsilon t - \frac{2}{9} \epsilon^2 t^2 \right] e^{i(\vec{k} \cdot \vec{x} + kt)} \quad (3.15)$$

Where,

$$\tilde{g} = m_a^L f(\epsilon) \mathcal{A}_0 \int_{g_{a\gamma\gamma}^L}^{g_{a\gamma\gamma}^M} g_{a\gamma\gamma} \tilde{p}(g_{a\gamma\gamma}) dg_{a\gamma\gamma}, \quad f(\epsilon) = p(m_a^L) \epsilon \quad (3.16)$$

The dimensionless parameters a_1 and a_2 are defined as follows,

$$a_1 = 1 + \epsilon \left(\frac{1}{m_a^L} + \frac{p'(m_a^L)}{p(m_a^L)} \right) + \frac{2\epsilon^2}{3} \left(\frac{2p'(m_a^L)}{m_a^L p(m_a^L)} + \frac{p''(m_a^L)}{p(m_a^L)} \right), \quad a_2 = 1 + \frac{4\epsilon}{3} \left(\frac{1}{m_a^L} + \frac{p'(m_a^L)}{p(m_a^L)} \right) \quad (3.17)$$

The power carried by the echo wave is given by,

$$P_N^\epsilon = 2N\mathcal{Z}(\epsilon, t) \left[P_{N=1} \right]_{g_{a\gamma\gamma}^M} \quad (3.18)$$

Where,

$$\mathcal{Z}(\epsilon, t) = f(\epsilon) \left[\int_{g_{a\gamma\gamma}^L}^{g_{a\gamma\gamma}^M} \frac{g_{a\gamma\gamma}}{g_{a\gamma\gamma}^M} \tilde{p}(g_{a\gamma\gamma}) dg_{a\gamma\gamma} \right]^2 \left[a_1 + \frac{\epsilon}{m_a^L} a_2 \right]^{-1} \left[a_1^2 + \frac{7}{24} \left(a_2^2 - \frac{12}{7} a_1 \right) \epsilon^2 t^2 \right] \quad (3.19)$$

Here, $P_{N=1}$ refers to the power in the original, single ALP case. We now apply our results to a few specific cases.

3.2 All masses and couplings equal

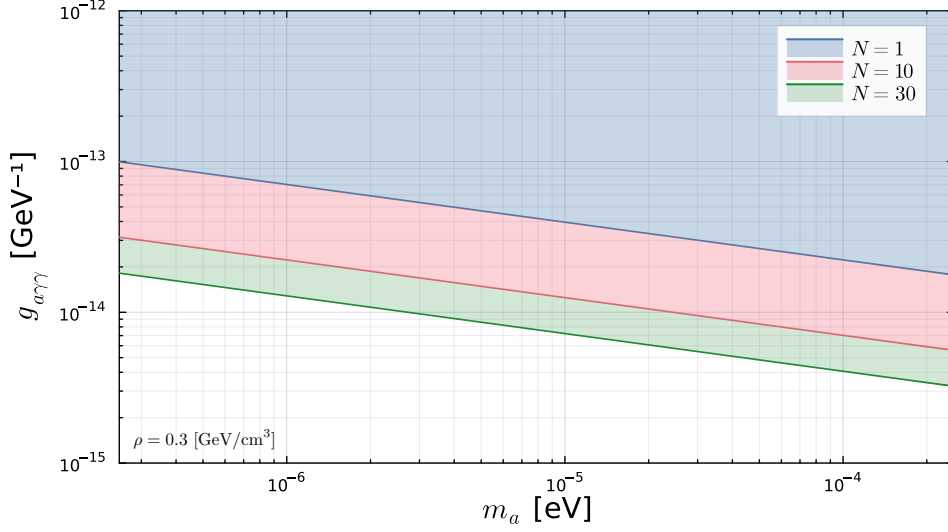


Figure 2. Projected constraints for $N = 10$ and $N = 30$ ALPs compared to the single ALP case for the isothermal model with $\rho = 0.3$ [GeV/cm³].

The simplest possible case occurs when all the ALPs have the same mass and coupling strengths, equal to $g_{a\gamma\gamma}$ and m_a . The easiest approach is to start from our general differential equation which simplifies greatly in this case,

$$(\partial_t^2 + p^2)\vec{A}_1^p = -iN\vec{B}_{kp}\left[e^{i(m_a-p)t} + e^{-i(m_a+p)t}\right] \quad (3.20)$$

It is clear from this that the amplitude of the echo wave is,

$$\vec{A}(t, \vec{x}) = \vec{a}_0 e^{i(\vec{k}\cdot\vec{x}-kt)} - N\frac{g}{4}t(\hat{k} \times \vec{a}_0)e^{i(\vec{k}\cdot\vec{x}+kt)} \quad (3.21)$$

That is, the magnitude of the echo wave will be amplified N times. To estimate the power, we first note that,

$$\rho = \frac{1}{2} \sum_{n=1}^N (m_a^n)^2 \mathcal{A}_0^2 = \frac{N}{2} m_a^2 \mathcal{A}_0^2 \quad (3.22)$$

Then, the power becomes,

$$P_N = NP_{N=1} = Ng_{a\gamma\gamma}^2 \frac{t}{16} \rho \frac{dP_0}{d\nu} \Big|_{k=m_a/2} \quad (3.23)$$

We can also derive this result by considering the limits of our results in subsection 3.1. To start with, note that we cannot simply take the limit $\epsilon \rightarrow 0$, since this collapses the integral in $Q(t)$ to 0. We also need to consider the variation of the probability distribution. To see this, consider the Taylor expanded integral,

$$Q(t) \Big|_{m_a^M=m_a^L+2\epsilon} = 2m_a^L \cos(m_a^L t) p(m_a^L) \epsilon \left[1 + \epsilon \left(\frac{1}{m_a^L} + \frac{p'(m_a^L)}{p(m_a^L)} \right) + \dots \right] \quad (3.24)$$

We require that this simply equal $m_a \cos(m_a t)$ in the required limit. This happens if,

$$\lim_{\epsilon \rightarrow 0} \epsilon p(m_a) = \frac{1}{2} \quad (3.25)$$

Essentially, while the integral limits do collapse to a single point ($m_a^L = m_a$ since all the masses are equal), we must make sure that the probability distribution also peaks in exactly the right manner so that the normalisation condition holds true. Further, since all the coupling strengths are also equal, $\tilde{p}(g_{a\gamma\gamma})$ simply becomes a delta distribution. If we proceed as above, we find,

$$\lim_{\epsilon \rightarrow 0} : a_1 = 1, a_2 = 1, \tilde{g} = \frac{1}{2} m_a g_{a\gamma\gamma} \mathcal{A}_0, \mathcal{Z}(\epsilon, t) = \frac{1}{2} \quad (3.26)$$

Therefore,

$$\vec{A}(t, \vec{x}) = \vec{a}_0 e^{i(\vec{k} \cdot \vec{x} - kt)} - N \frac{g}{4} t (\hat{k} \times \vec{a}_0) e^{i(\vec{k} \cdot \vec{x} + kt)}, P_N = N P_{N=1} \quad (3.27)$$

This is exactly as we derived before. Thus, the power is amplified by a factor of N compared to the single ALP case, denoted by $P_{N=1}$. This can be potentially observationally significant. The bounds obtained in figure 1 improve as N increases as shown in figure 2. Reference [37] highlights an $N = 30$ case in their work which we also show in the above figure. Mathematically, this case is akin to making the transformation $g \rightarrow \sqrt{N}g$ - that is, it is equivalent to the scenario where we only have one ALP but with a coupling that is \sqrt{N} times larger than earlier.

3.3 Variable couplings and all masses equal

The next case we consider is when all the ALPs have the same mass, m_a , but variable coupling strengths. As noted previously, the coupling strength distribution does not affect the dynamics of the situation. We take the mass distribution limit as was described in the last subsection to get,

$$\lim_{\epsilon \rightarrow 0} : a_1 = 1, a_2 = 1, \tilde{g} = \frac{1}{2} m_a \langle g_{a\gamma\gamma} \rangle \mathcal{A}_0, \mathcal{Z}(\epsilon, t) = \frac{\langle g_{a\gamma\gamma} \rangle^2}{2(g_{a\gamma\gamma}^M)^2} \quad (3.28)$$

The solution is straightforward,

$$\vec{A}(t, \vec{x}) = \vec{a}_0 e^{i(\vec{k} \cdot \vec{x} - kt)} - N \frac{m_a \langle g_{a\gamma\gamma} \rangle \mathcal{A}_0}{4} t (\hat{k} \times \vec{a}_0) e^{i(\vec{k} \cdot \vec{x} + kt)} \quad (3.29)$$

As with the previous case, the echo signal is amplified this time as well - the strength of the amplification depends on the exact choice of the coupling strengths. The echo wave power can be written down as,

$$P_N = N \langle g_{a\gamma\gamma} \rangle^2 \frac{t}{16} \rho \frac{dP_0}{d\nu} \Big|_{k=m_a/2} \quad (3.30)$$

For the sake of simplicity, we assume that the coupling distribution is uniform over the given range and that $g_{a\gamma\gamma}^M \gg g_{a\gamma\gamma}^L$. Then,

$$P_N = \frac{1}{4} N (g_{a\gamma\gamma}^M)^2 \frac{t}{16} \rho \frac{dP_0}{d\nu} \Big|_{k=m_a/2} \quad (3.31)$$

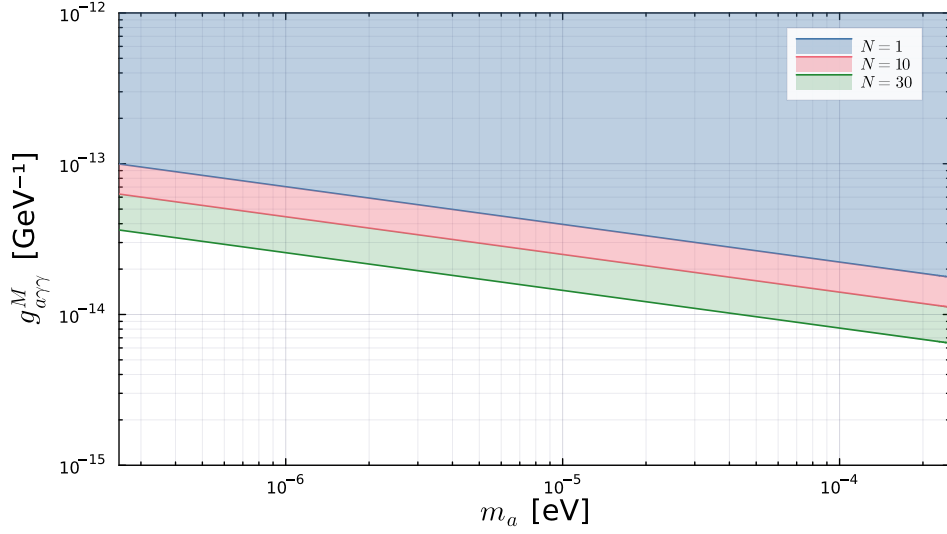


Figure 3. Projected constraints for $N = 10$ and $N = 30$ ALPs with all masses equal compared to the single ALP case for the isothermal model with $\rho = 0.3$ [GeV/cm³].

The equation above is mathematically equivalent to a single ALP case with $g \rightarrow \sqrt{N}g_M/2$. As shown in figure 3, the constraints from the previous case are a bit weaker as a result. The advantage of this treatment is that even for multiple ALPs with differing couplings, we do not need to know the exact distribution of coupling strengths. Starting off with a set of N different coupling strengths, we have derived an answer that depends on, at most, two free coupling parameters. A general idea of the limits of the parameter space being searched for is sufficient to provide a good idea of the kind of signal we expect - this, in turn, can help focus our experimental probes towards the most promising regions of the parameter space.

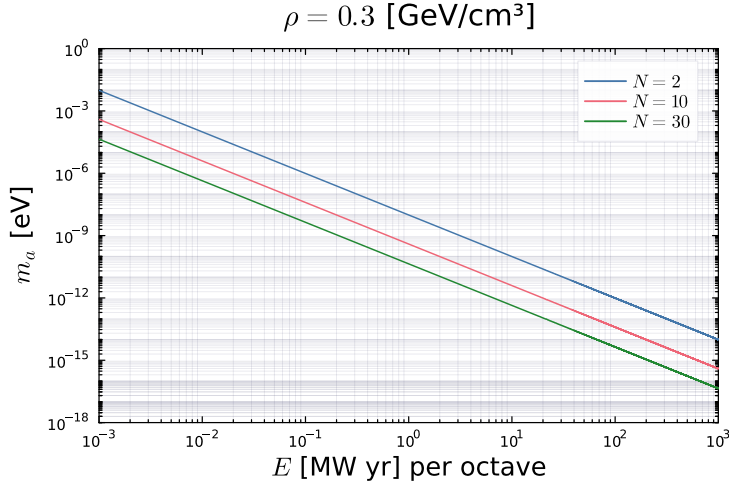


Figure 4. Range of masses that can be probed depending on outgoing wave energy in the the isothermal model for different N .

A second interesting application is as follows. If we assume, for example, $g_{a\gamma\gamma}^M \sim 10^{-12}$ [GeV $^{-1}$] based on existing constraints, the above equation gives us a range of masses that we can probe depending on the energy of the outgoing photon wave. This is shown in figure 4. This establishes a direct connection between the input power and the ALP mass and can serve as a sensitivity estimate - for a given range of ALP masses, we can estimate the rough power needed to produce a detectable signal. As before, this is significant especially in such a multi-ALP context where we have shown that an “effective” coupling strength allows us to determine the features of the expected signal without knowing the exact details of the mass and coupling distribution.

3.4 Variable masses and all couplings equal

As a straightforward illustration of our results to a more complicated case, let us consider a situation where the mass distribution is uniform (but narrow), while all of the coupling strengths are same and equal to $g_{a\gamma\gamma}$ (where $g_{a\gamma\gamma}$ now refers to a specific value for the coupling strength rather than the dummy integration variable as used above). Then, we have,

$$\tilde{p}(g'_{a\gamma\gamma}) = \delta(g'_{a\gamma\gamma} - g_{a\gamma\gamma}), \quad p(m_a) = \frac{1}{m_a^M - m_a^L} = \frac{1}{2\epsilon}, \quad p'(m_a) = 0, \quad p''(m_a) = 0 \quad (3.32)$$

Then,

$$a_1 = 1 + \frac{\epsilon}{m_a^L}, \quad a_2 = 1 + \frac{4\epsilon}{3m_a^L} \quad (3.33)$$

We express our answer in a more dimensionless form by redefining $\epsilon \rightarrow \epsilon m_a^L$. We find,

$$\vec{A}(t, \vec{x}) = \vec{a}_0 e^{i(\vec{k} \cdot \vec{x} - kt)} - N \frac{g_{a\gamma\gamma} m_a^L \mathcal{A}_0 t}{4} (\hat{k} \times \vec{a}_0) \left[1 + \epsilon + i \frac{m_a^L t}{2} \left(1 + \frac{4}{3} \epsilon \right) \epsilon - \frac{2(m_a^L t)^2}{9} \epsilon^2 \right] e^{i(\vec{k} \cdot \vec{x} + kt)} \quad (3.34)$$

We also have,

$$P_N^\epsilon = N \left[1 + 2\epsilon + \frac{4}{3} \epsilon^2 \right]^{-1} \left[(1 + \epsilon)^2 - \frac{5(m_a^L t)^2}{24} \epsilon^2 \left(1 - \frac{4}{3} \epsilon - \frac{112}{45} \epsilon^2 \right) \right] P_{N=1} \quad (3.35)$$

The echo wave is amplified again in this case. Aside from the usual N amplification, we have an additional enhancement depending on the exact difference between the masses and the timescale under consideration. For larger times, the higher degree polynomial terms will dominate with the caveat that we will also be approaching the region where the perturbation theory treatment will break down. Technically, the condition for the validity of the perturbative treatment requires,

$$\epsilon m_a^L t = 1 \Rightarrow t = \frac{2}{m_a^M - m_a^L} \quad (3.36)$$

In this limit, higher order terms will also contribute, but the coefficients of these terms will get successively smaller, and the major contribution is already captured by the terms considered here. For masses on the scale of 10^{-4} [eV], for instance, this would amount to a timescale of $t \sim 10^{-11}$ [sec]. This is a short timescale and according to the answer we

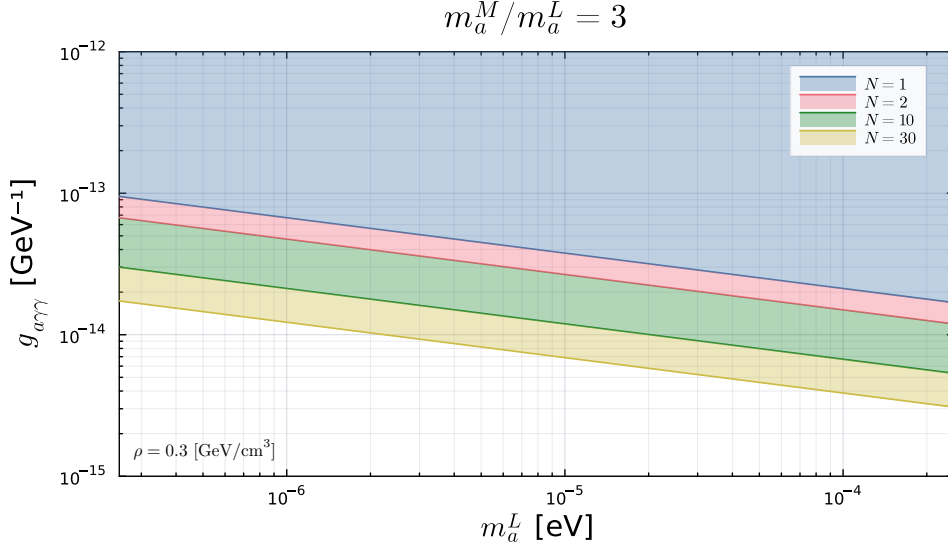


Figure 5. Constraints with $N = 2$, $N = 10$, $N = 30$ and mass ratio 3 corresponding to $\epsilon = 1$ for the isothermal model with $\rho = 0.3$ [GeV/cm³].

have derived, it is possible that the echo wave is amplified significantly on this timescale. As mentioned earlier, we replace t by R/v_\perp in order to arrive at a rough experimental estimate. Since this value is much larger than the timescale of amplification ($\sim 10^{-11}$ [sec]), we should be able to detect such echo signals.

Consider a situation with $m_a^L t \sim 1$. Our perturbative answer will be valid for any $\epsilon \leq 1$, in this case. The power will be,

$$\begin{aligned}
 P_N^\epsilon &= N \left[1 + 2\epsilon + \frac{4}{3}\epsilon^2 \right]^{-1} \left[(1 + \epsilon)^2 - \frac{5}{24}\epsilon^2 \left(1 - \frac{4}{3}\epsilon - \frac{112}{45}\epsilon^2 \right) + \frac{131}{1620}\epsilon^4 \right] P_{N=1} \\
 &\leq P_N^{\epsilon=1} \approx 1.1NP_{N=1}
 \end{aligned} \tag{3.37}$$

This corresponds to a straightforward additional amplification of 10% aside from the usual N amplification. The projected bounds for this maximal case are plotted in figure 5 for the maximal case with $\epsilon = 1$ for $N = 2$, $N = 10$ and $N = 30$. As we can see, there is an enhancement in the projected bounds even for the $N = 2$ case compared to the single ALP scenario. As expected, higher N leads to more area of the parameter space being covered.

The projected bounds that we show here fall in an area of the parameter space that is mostly unconstrained and can, therefore, be an interesting potential avenue for constraining such ALPs. The mass range considered here is given by $m_a^L \in [2.5 \times 10^{-7}, 2.5 \times 10^{-3}]$ [eV] aligning with the transparency window of the earth's atmosphere which is almost completely transparent to photons in this frequency range (around 0.3 – 30 [GHz]). This mass range also corresponds to QCD axions and therefore, these results can be used to provide stronger or complementary bounds compared to the traditional haloscope based experiments like ADMX [45–51] and CAPP [52–55]. However, our results apply, in general,

to any mass range (as long as the perturbative condition is valid). As such, in principle, our results could also be extended to obtain newer and complementary bounds on ALPs in lower mass ranges, 10^{-10} [eV] $< m_a^L < 10^{-6}$ [eV], which have been investigated using data from Chandra and Fermi-LAT which are not ground-based and are, therefore, not constrained to work only in the earth’s transparent window.

There are also future proposals that would enable us to look at extremely low frequency regimes. Two such proposals are NASA’s FARSIDE concept [56, 57] and the DSL (Discovering the Sky at the Longest wavelengths) experiment [58] in China, both of which are based on the farside of the moon. The FARSIDE experiment will be designed as an array of low-frequency antennas on the lunar farside surface, while the DSL experiment will include a set of satellites in the lunar orbit on the farside. Both these experiments will be designed to detect ultra-low frequency signals below 30 MHz with both aiming for a minimum frequency of around 100 kHz. For example, the DSL experiment proposes a set of detectors with radius 0.5 m, this gives us a lower value of $R/v_\perp \sim 10^{-4}$ [sec] for the caustic ring model and 10^{-6} [sec] for the isothermal model both of which are still several orders of magnitude higher than the timescale we require for the perturbative regime to be valid. However, the major issue in such a situation is with the question of sending out photons of such low energy reliably in a direction of our choosing. For a start, such beams can only be sent out using satellite-based methods because otherwise the earth’s atmosphere will not allow them to pass through. Further, in order to transmit such large wavelengths, the required antennae will also need to be very large. For example, on the earth, very low frequency transmitters use wire antennae that go up to several kilometres long, which, in the context of satellites, seems impractical. These issues, however, could be potentially resolved in the future based on novel technological advancements. Here, we note that while our results can be applied to these scenarios in principle, the practicality of the experimental methods is unclear.

4 The incoherent scenario

As mentioned earlier, the most general form of the ALP fields includes an additional random phase factor. In this section, we take a look at what happens in such a situation. We have,

$$(\partial_t^2 + p^2)\vec{A}_1^p = -i\mathcal{A}_0(\vec{p} \times \vec{a}_0)\delta^{(3)}(\vec{k} - \vec{p})e^{-ipt}\sum_{n=1}^N g_{a\gamma\gamma}^n m_a^n \cos(m_a^n t + \theta_n) \quad (4.1)$$

In general, averaging over the random phase on the RHS makes the drive term vanish. Instead, we focus on replacing the randomised sum with an “effective” driving term by using the root mean square value, similar to how we treat random walks. This difference in treatment underscores the important fact that the two cases - coherent and incoherent - are not equivalent to each other in any limiting sense. They are separate, distinct scenarios that must be treated separately. As before, we start from the general case and then consider a few specific cases to illustrate the broad reach of our results.

4.1 Incoherent scenario for general distributions

We start with,

$$(\partial_t^2 + p^2)\vec{A}_1^p = -i\mathcal{A}_0(\vec{p} \times \vec{a}_0)\delta^{(3)}(\vec{k} - \vec{p})e^{-ipt} \sum_{n=1}^N g_{a\gamma\gamma}^n m_a^n \cos(m_a^n t + \theta_n) \quad (4.2)$$

Our assumptions from the previous section still hold true with the additional information that θ_n also forms a similar set of identically distributed random variables according to some distribution. In general, we expect such a distribution to be uniform in the range $[0, 2\pi]$ since there is no specific choice of phase. This means, for large N ,

$$\begin{aligned} (\partial_t^2 + p^2)\vec{A}_1^p &= -\frac{i}{2\pi} N \mathcal{A}_0(\vec{p} \times \vec{a}_0)\delta^{(3)}(\vec{p} - \vec{k})e^{-ipt} \int_{g_{a\gamma\gamma}^L}^{g_{a\gamma\gamma}^M} g_{a\gamma\gamma} \tilde{p}(g_{a\gamma\gamma}) dg_{a\gamma\gamma} \\ &\quad \times \int_{m_a^L}^{m_a^M} \int_0^{2\pi} m_a \cos(m_a t + \theta) p(m_a) dm_a d\theta \end{aligned} \quad (4.3)$$

Clearly, the θ integral vanishes - in other words, the random fluctuations in the phase average out to zero over the entire interval. Therefore, we consider a different approach based on arguments similar to random walks. Instead of considering the average “displacement”, we consider the average “distance” when treating random walks and in the same spirit, we move forward with the root mean square value here as well. In general, consider,

$$\sum_{n=1}^N g_{a\gamma\gamma}^n m_a^n \cos(m_a^n t + \theta_n) = \text{Re} \left\{ \sum_{n=1}^N g_{a\gamma\gamma}^n m_a^n e^{i(m_a^n t + \theta_n)} \right\} = \text{Re}\{Z_N\} = |Z_N| \cos[\Phi(t)] \quad (4.4)$$

Therefore, the amplitude of our effective drive term is given by $|Z_N|$. Here, $\Phi(t)$ is some phase factor composed of some combination of m_a^n and θ_n . Now,

$$|Z_N|^2 = \sum_{n=1}^N (g_{a\gamma\gamma}^n m_a^n)^2 + \frac{1}{2} \sum_{n \neq m}^N g_{a\gamma\gamma}^n g_{a\gamma\gamma}^m m_a^n m_a^m e^{i(\theta_n - \theta_m)} \quad (4.5)$$

The second term will average out to zero here. Thus,

$$|Z_N| \sim \sqrt{\sum_{n=1}^N (g_{a\gamma\gamma}^n m_a^n)^2} \quad (4.6)$$

Based on this, we approximate eq. (4.2) as,

$$(\partial_t^2 + p^2)\vec{A}_1^p = -i\mathcal{A}_0(\vec{p} \times \vec{a}_0)\delta^{(3)}(\vec{k} - \vec{p})e^{-ipt} \sqrt{\sum_{n=1}^N (g_{a\gamma\gamma}^n m_a^n)^2} \cos(m_a^* t + \Theta) \quad (4.7)$$

Where,

$$m_a^* = \int_{m_a^L}^{m_a^M} m_a p(m_a) dm_a \quad (4.8)$$

Here, Θ is a global phase factor that we drop from our calculation. In other words, we replace the sum of random drive terms by a single, effective drive term with an amplitude as estimated above and a single mode of oscillation depending on m_a^* . Crucially, our approximation will only be valid for drive terms that are closely spaced in frequency space - in other words, the string of cosine terms in our initial equation must be closely spaced. This implies that the ALP masses are closely spaced, i.e., the mass splitting parameter, defined as $m_a^M - m_a^L = 2\epsilon$ as before, is small (i.e., $\epsilon \ll m_a^L$). We finally have,

$$(\partial_t^2 + p^2)\vec{A}_1^p = -2i\vec{D}_{kp}^N e^{-ipt} \cos(m_a^* t) \quad (4.9)$$

Here,

$$\vec{D}_{kp}^N = \frac{\mathcal{A}_0}{2}(\vec{p} \times \vec{a}_0)\delta^{(3)}(\vec{k} - \vec{p})\sqrt{\sum_{n=1}^N (g_{a\gamma\gamma}^n m_a^n)^2} \quad (4.10)$$

This equation is exactly similar to the one we encountered in the single ALP case with m_a replaced by m_a^* . The resonant condition is given by,

$$p = \frac{1}{2}m_a^* = \frac{1}{2} \int_{m_a^L}^{m_a^M} m_a p(m_a) dm_a \quad (4.11)$$

The resonant solution is given by,

$$\vec{A}(t, \vec{x}) = \vec{a}_0 e^{i(\vec{k} \cdot \vec{x} - kt)} - \frac{\mathcal{A}_0 t}{4} \sqrt{\sum_{n=1}^N (g_{a\gamma\gamma}^n m_a^n)^2} (\hat{k} \times \vec{a}_0) e^{i(\vec{k} \cdot \vec{x} + kt)} \quad (4.12)$$

The power carried by the echo wave is given by,

$$P_N = \left[\int_{g_{a\gamma\gamma}^L}^{g_{a\gamma\gamma}^M} g_{a\gamma\gamma}^2 \tilde{p}(g_{a\gamma\gamma}) dg_{a\gamma\gamma} \right] \left. \frac{\rho t}{16} \frac{dP_0}{d\nu} \right|_{p=m_a^*/2} \quad (4.13)$$

Therefore, we see that the incoherent case clearly removes the earlier N dependence from the power. Another interesting point to note is that, unlike earlier, the mass distribution does not affect the power itself in any way. It simply influences the resonant condition, but the power itself is unaffected by what kind of distribution of masses we have. We can also express the power as,

$$P_N = f_g \left[P_{N=1} \right]_{p=m_a^*/2}^{g_{a\gamma\gamma}^M} \quad (4.14)$$

Here,

$$f_g = \int_{g_{a\gamma\gamma}^L}^{g_{a\gamma\gamma}^M} \left(\frac{g_{a\gamma\gamma}}{g_{a\gamma\gamma}^M} \right)^2 \tilde{p}(g_{a\gamma\gamma}) dg_{a\gamma\gamma} \leq 1 \quad (4.15)$$

The above integral is always less than unity for any smooth distribution - in fact, it is only equal to unity in the extreme case of a delta function (i.e., all couplings equal). This essentially means that the incoherent case always leads to a weaker signal compared to even the single ALP scenario. In fact, it can only approach the single ALP case as an extreme limit. Clearly, this has significant potential ramifications for interpreting experimental results whose conclusions will depend crucially on the underlying framework (single or multiple ALP) considered. We illustrate this point even more clearly in the following specific cases.

4.2 All masses equal

We proceed as we did in the coherent case. The resonant condition becomes,

$$p = \frac{1}{2} \lim_{\epsilon \rightarrow 0} \int_{m_a}^{m_a+2\epsilon} m \delta(m - m_a) dm = \frac{1}{2} m_a \quad (4.16)$$

As discussed earlier, the function $f(r_g)$ becomes unity in this case. The solution is given by,

$$\vec{A}(t, \vec{x}) = \vec{a}_0 e^{i(\vec{k} \cdot \vec{x} - kt)} - \frac{gt}{4} (\hat{k} \times \vec{a}_0) e^{i(\vec{k} \cdot \vec{x} + kt)} \quad (4.17)$$

Where $g = g_{a\gamma\gamma} m_a \mathcal{A}_0$ as defined earlier. The power is,

$$P_N = P_{N=1} \quad (4.18)$$

This is exactly the same as the single ALP case. The general feature of the incoherent case is the marked absence of the N dependent amplification that we had earlier. Observationally, this means that we cannot differentiate between such a scenario and the single ALP case. However, this only happens in the extreme case when all of the masses and couplings are equal. As an offshoot of this case, let us consider the situation where the couplings are still equal, but the masses are not. The resonant condition becomes,

$$\begin{aligned} p = \frac{1}{2} \int_{m_a^L}^{m_a^L+2\epsilon} m_a p(m_a) dm_a &= \epsilon p(m_a^L) m_a^L \left[1 + \epsilon \left(\frac{1}{m_a^L} + \frac{p'(m_a^L)}{p(m_a^L)} \right) \right. \\ &\quad \left. + \frac{2\epsilon^2}{3} \left(\frac{2p'(m_a^L)}{m_a^L p(m_a^L)} + \frac{p''(m_a^L)}{p(m_a^L)} \right) \right] + \dots = m_a^L f(\epsilon) a_1 + \dots \end{aligned} \quad (4.19)$$

Here, $f(\epsilon)$ and a_1 are as defined in eqs. (3.16) and (3.17). Now, the normalisation condition for the masses can be expressed as,

$$\int_{m_a^L}^{m_a^L+2\epsilon} p(m) dm = 2f(\epsilon) \left[1 + \frac{p'(m_a^L)}{p(m_a^L)} \epsilon + \frac{2p''(m_a^L)}{3p(m_a^L)} \epsilon^2 + \dots \right] = 1 \Rightarrow f(\epsilon) = \frac{1}{2} + \mathcal{O}(\epsilon^2) \quad (4.20)$$

Therefore, the resonant condition is,

$$p = \frac{1}{2} m_a^L + \mathcal{O}(\epsilon^2) \quad (4.21)$$

While our resonance condition looked formidable initially, we have reduced it to a more tractable and experimentally relevant form. The power is simply,

$$P_N = P_{N=1} \quad (4.22)$$

Therefore, both these cases reduce, in leading order, to the single ALP scenario.

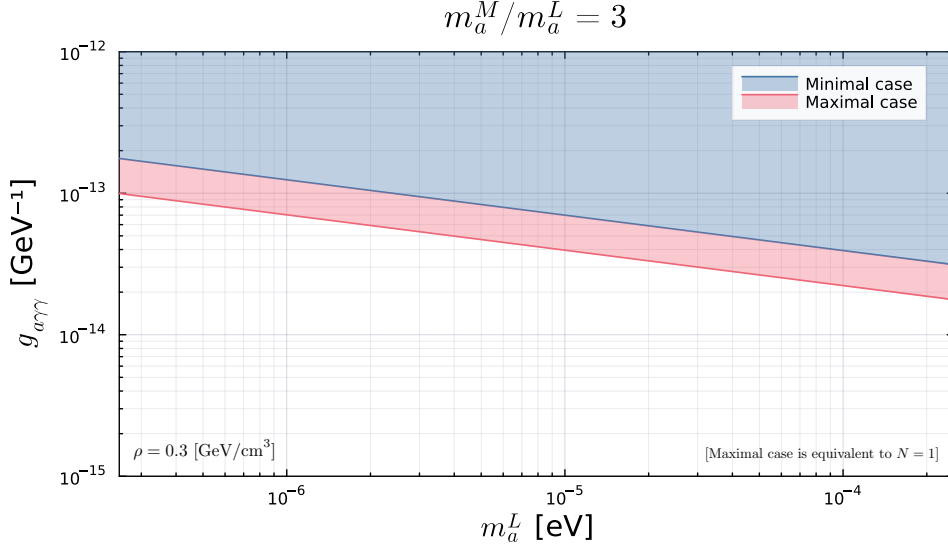


Figure 6. Projected constraints for the minimal and maximal cases for the incoherent scenario with variable couplings in the isothermal model with $\rho = 0.3$ [GeV/cm³].

4.3 Variable couplings and all masses equal

The next simplest case is when the masses are all equal, but the couplings are not. The resonant condition is simply $p = m_a/2$ as before. The solution is,

$$\vec{A}(t, \vec{x}) = \vec{a}_0 e^{i(\vec{k} \cdot \vec{x} - kt)} - \frac{m_a \langle g_{a\gamma\gamma} \rangle \mathcal{A}_0}{4} t (\hat{k} \times \vec{a}_0) e^{i(\vec{k} \cdot \vec{x} + kt)} \quad (4.23)$$

As with the previous case, the echo signal is modified this time as well - the deviation from the single ALP scenario depends on the exact choice of the coupling strengths. The echo wave power can be written down as,

$$P_N = f_g \left[P_{N=1} \right]_{g_{a\gamma\gamma}^M} = \langle g_{a\gamma\gamma} \rangle^2 \frac{t}{16} \rho \frac{dP_0}{d\nu} \Big|_{k=m_a/2} \quad (4.24)$$

For uniform coupling distributions,

$$P_N = \frac{1}{3} \left[\left(1 + \frac{g_{a\gamma\gamma}^L}{g_{a\gamma\gamma}^M} \right)^2 - \frac{g_{a\gamma\gamma}^L}{g_{a\gamma\gamma}^M} \right] \left[P_{N=1} \right]_{g_{a\gamma\gamma}^M} \quad (4.25)$$

Once again, we have reduced the answer to two free “effective” couplings instead of N different ones. Clearly,

$$\frac{1}{3} \left[P_{N=1} \right]_{g_{a\gamma\gamma}^M} \leq P_N = f_g \left[P_{N=1} \right]_{g_{a\gamma\gamma}^M} \leq \left[P_{N=1} \right]_{g_{a\gamma\gamma}^M} \quad (4.26)$$

As before, the projected sensitivities are weaker compared to the single ALP scenario. The exact sensitivities are dependent on the kind of coupling strength distribution in the underlying model. For uniform distributions, the maximal case corresponds to the single

ALP scenario, while the minimal case corresponds to a third of it. The actual power, in any given situation, lies between this. This situation is depicted in figure 6. This result, while strikingly different from the coherent case, is as important and can potentially play a major role in interpreting experimental results.

5 Discussions

In this manuscript, we have considered the case of echoes in the context of multiple ALPs interacting with photons. We have briefly revisited and cast the arguments presented in earlier literature into a more tractable form and extended the formalism to cover the case of multiple ALPs. We have derived initial results for general distributions for both coherent and incoherent configurations and further, considered various cases systematically - when the masses and couplings are all equal, when only the masses are equal and when only the couplings are equal. Our derivations have been presented in detail in the supplementary materials.

Specifically, we have shown that, in the coherent case with all ALP fields oscillating “in phase”, the power scales as N leading to a sharper amplification of the echo signal and strengthening the projected bounds depending on how large N is. In case of small mass splittings between the ALPs, we have also shown that the mass splitting parameter itself provides an additional amplification. Such an amplification results in stronger sensitivities compared to the single ALP case. When discussing the incoherent case in section 4, we have shown how similar cases lead to a suppression of the observable signal leading to weaker projected bounds. Both the coherent and incoherent cases are, therefore, important for the proper interpretation of future experimental results. We also discuss how our study, originally in the context of the QCD axion mass range, might also be applicable to other mass ranges, including the ultra-low frequency ranges that will be probed by future experiments, specifically NASA’s FARSIDE and the DSL experiment in China. While sending out such low frequency photons into space in order to generate echoes might be impractical, our universe is already teeming with photons at these energies coming from various astrophysical sources including galactic emissions and even the Cosmic Microwave Background. Following the approach laid down in reference [29] and the groundwork in this manuscript, a detailed analysis of echoes generated from such galactic and extra-galactic sources at these ultra-light frequencies can be performed. Such studies could provide complementary bounds to existing data, for example, like those recently explored in references [59–61].

More detailed and non-uniform probability distributions could still be effectively approximated by a smooth, uniform distribution if the mass range is quite narrow (which is similar to the case we considered) or if the variation in the masses is slow. In multiple ALP models, for example utilising the clockwork mechanism, the ALP masses are usually given by [35],

$$m_n^2 = m^2 \left[q^2 + 1 - 2q \cos \left(\frac{n\pi}{N+1} \right) \right] \quad (5.1)$$

The masses follow an approximately uniform distribution if q is large enough; the relative spacing between the masses is $\mathcal{O}(1/q)$ rendering such a treatment valid. The concept of an axion iceberg or a single broad signal which arises in such ALPs with very small mass splittings in the context of hadron colliders was recently explored in reference [36]. Our treatment of the echoes in sections 3 and 4 would pertain to such situations and could provide complementary avenues for probing such beyond-standard-model scenarios. Some string theory models also generate ALP masses using a logarithmic distribution [32],

$$P(m) \sim \ln \left(\frac{m}{M_{Pl}} \right) \quad (5.2)$$

For ALPs with small mass splittings, such a distribution varies slowly enough to be approximated by a uniform distribution. While more detailed ALP setups would have more complicated mass spectra depending on the exact model, our results in the uniform case still hold qualitatively and are interesting due to the observational appeal and the analytical tractability. Further, our results are general and can be applied to these cases properly, if required. Our study could provide a blueprint for more detailed model dependent calculations in this context and their implications which will be explored in a future work.

A Standard solution of a forced oscillator

We start with,

$$(\partial_t^2 + p^2)\vec{A}_1^p = -2i\vec{B}_{kp}e^{-ipt}\cos(m_at) \quad (A.1)$$

The homogenous equation is,

$$(\partial_t^2 + p^2)\vec{A}_1^p = 0 \quad (A.2)$$

This has two straightforward linearly independent solutions,

$$\vec{u}_1 = \vec{a}e^{ipt}, \quad \vec{u}_2 = \vec{b}e^{-ipt} \quad (A.3)$$

The Wronskian can be computed as,

$$\mathcal{W} = -2ip \quad (A.4)$$

The particular solution can then be written as,

$$\vec{u}_p = \frac{i}{2p}e^{-ipt} \int_0^t d\xi \vec{G}(\xi) e^{ip\xi} - \frac{i}{2p}e^{ipt} \int_0^t d\xi \vec{G}(\xi) e^{-ip\xi} \quad (A.5)$$

Here, $\vec{G}(t)$ is the inhomogenous term in our equation,

$$\vec{G}(t) = -2i\vec{B}_{kp}e^{-ipt}\cos(m_at) \quad (A.6)$$

The first integral gives us,

$$\int_0^t d\xi \vec{G}(\xi) e^{ip\xi} = -2i\vec{B}_{kp} \int_0^t d\xi \cos(m_a\xi) = -2i\vec{B}_{kp} \frac{\sin(m_at)}{m_a} \quad (A.7)$$

Similarly, the second integral gives us,

$$\int_0^t d\xi \vec{G}(\xi) e^{-ip\xi} = -2i\vec{B}_{kp} \int_0^t d\xi \cos(m_a \xi) e^{-2ip\xi} = -\vec{B}_{kp} \left[\frac{e^{i(m_a-2p)t} - 1}{m_a - 2p} - \frac{e^{-i(m_a+2p)t} - 1}{m_a + 2p} \right] \quad (\text{A.8})$$

Or,

$$\int_0^t d\xi \vec{G}(\xi) e^{-ip\xi} = -\vec{B}_{kp} \left[\frac{e^{i(m_a-2p)t}}{m_a - 2p} - \frac{e^{-i(m_a+2p)t}}{m_a + 2p} - \frac{4p}{(m_a - 2p)(m_a + 2p)} \right] \quad (\text{A.9})$$

Therefore,

$$\vec{u}_p = \frac{i}{m_a} \vec{B}_{kp} \left[\frac{e^{i(m_a-p)t}}{m_a - 2p} + \frac{e^{-i(m_a+p)t}}{m_a + 2p} - \frac{2m_a e^{ipt}}{(m_a - 2p)(m_a + 2p)} \right] \quad (\text{A.10})$$

Now, imposing the initial conditions $\vec{A}_1^p(t=0) = 0$, $\dot{\vec{A}}_1^p(t=0) = 0$, we get,

$$\vec{a} = \vec{b} = 0 \quad (\text{A.11})$$

Therefore, the complete solution is,

$$\vec{A}_1^p = \frac{i}{m_a} \vec{B}_{kp} \left[\frac{e^{i(m_a-p)t}}{m_a - 2p} + \frac{e^{-i(m_a+p)t}}{m_a + 2p} - \frac{2m_a e^{ipt}}{(m_a - 2p)(m_a + 2p)} \right] \quad (\text{A.12})$$

B Validity of large N approximation

In this section, we discuss the validity of some of the statistical aspects used in the calculations. We have two sets of N random variables, m_a^i and $g_{a\gamma\gamma}^i$, with $i \in [1, N]$. We assume that each $g_{a\gamma\gamma}^i$ and m_a^i is independently drawn from a continuous smooth distribution in a certain interval. We further assume that each $g_{a\gamma\gamma}^i \in [g_{a\gamma\gamma}^L, g_{a\gamma\gamma}^M]$ and $m_a^i \in [m_a^L, m_a^M] \forall i \in [1, N]$. The probability distribution for the coupling strengths is denoted by $\tilde{p}(g_{a\gamma\gamma})$ and the one for the ALP masses is $p(m_a)$. We also assume that the two distributions are independent of each other, i.e., uncorrelated. Now, the Law of Large Numbers can be expressed as the following theorem [62],

Theorem. *Let X_1, X_2, \dots, X_n be a sequence of independent random variables having a common distribution, and let $E[X_i] = \mu$. Then, with probability 1,*

$$\frac{1}{n} \sum_{i=1}^n X_i \rightarrow \mu \text{ as } n \rightarrow \infty$$

Based on this, let us look at the approximation we used in the main text,

$$\frac{1}{N} \sum_{n=1}^N g_{a\gamma\gamma}^n m_a^n \cos(m_a^n t) = \int_{g_{a\gamma\gamma}^L}^{g_{a\gamma\gamma}^M} dg_{a\gamma\gamma} \tilde{p}(g_{a\gamma\gamma}) \int_{m_a^L}^{m_a^M} dm_a p(m_a) [g_{a\gamma\gamma} m_a \cos(m_a t)] \quad (\text{B.1})$$

This is essentially the Law of Large Numbers written as,

$$\begin{aligned} \frac{1}{N} \sum_{i=1}^N f(X_i)g(Y_i) &\xrightarrow{\text{for large } N} \langle f(X_i)g(Y_i) \rangle = \int_{y_a}^{y_b} \int_{x_a}^{x_b} f(X_i)g(Y_i)\tilde{p}(X_i)p(Y_i) dX_i dY_i \\ &= \langle f(X_i) \rangle \langle g(Y_i) \rangle \end{aligned} \quad (\text{B.2})$$

Where we have implicitly assumed that the two distributions are independent of each other, i.e., uncorrelated. This occurs in the limit of very large N , ideally infinite. But our focus in this section is to look at the validity of the above for finite N - namely, how large do we need N for the above to be roughly true? For this, let us first consider a situation where we only have a single set of random variables,

$$\frac{1}{N} \sum_{i=1}^N f(X_i) \rightarrow \langle f(X_i) \rangle = \int_a^b f(X_i)\tilde{p}(X_i) dX_i \quad (\text{B.3})$$

A simple and intuitive condition to quantify the fluctuations in $\langle f(X_i) \rangle$ is to impose,

$$\sqrt{\frac{1}{N} \text{Variance}[f(X_i)]} \equiv \frac{1}{\sqrt{N}} \sigma_f \ll \varepsilon^{1/2} \langle f(X_i) \rangle \equiv \varepsilon^{1/2} \mu_f \quad (\text{B.4})$$

Where ε is a real number that determines the precision of our approximation. Essentially, we are demanding that the fluctuations from the mean, relative to the number of total ALP fields in the theory, is a small quantity - at least smaller than the mean. The parameter ε quantifies the precision of our approximation. Satisfying the condition for $\varepsilon = 1$ is the standard, base case, while satisfying it for even smaller values of ε hints at better validity. Our condition can also be expressed as,

$$N\varepsilon \gg \left(\frac{\sigma_f}{\mu_f} \right)^2 \quad (\text{B.5})$$

For our scenario, a straightforward generalisation gives,

$$N\varepsilon \gg \left(\frac{\sigma_{fg}}{\mu_f \mu_g} \right)^2 \quad (\text{B.6})$$

Where μ_g denotes the mean of $g(Y_i)$ with respect to its distribution and σ_{fg} is the standard deviation of the quantity $f(X_i)g(Y_i)$,

$$\sigma_{fg}^2 = \langle [f(X_i)g(Y_i)]^2 \rangle - \langle f(X_i)g(Y_i) \rangle^2 = \langle f(X_i)^2 \rangle \langle g(Y_i)^2 \rangle - \mu_f^2 \mu_g^2 \quad (\text{B.7})$$

We can express this as,

$$\sigma_{fg}^2 = (\sigma_f^2 + \mu_f^2)(\sigma_g^2 + \mu_g^2) - \mu_f^2 \mu_g^2 = \sigma_f^2 \sigma_g^2 + \mu_f^2 \sigma_g^2 + \mu_g^2 \sigma_f^2 \quad (\text{B.8})$$

Or,

$$\left(\frac{\sigma_{fg}}{\mu_f \mu_g} \right)^2 = \left(\frac{\sigma_f \sigma_g}{\mu_f \mu_g} \right)^2 + \left(\frac{\sigma_f}{\mu_f} \right)^2 + \left(\frac{\sigma_g}{\mu_g} \right)^2 \quad (\text{B.9})$$

Let us identify $\{Y_i\}$ with the ALP masses and $\{X_i\}$ with the coupling strengths. In the main text, we focused on scenarios where the ALP masses were concentrated in a narrow range. Therefore,

$$\mu_g = \int_{y_a}^{y_a+\epsilon} dy g(y)p(y) = g(y_a) + g'(y_a) \int_{y_a}^{y_a+\epsilon} dy (y - y_a)p(y) + \dots \quad (\text{B.10})$$

The second term in the equation above is $\mathcal{O}(\epsilon)$ and the terms following it get successively smaller. In fact,

$$\sigma_g^2 = \int_{y_a}^{y_a+\epsilon} dy g(y)^2 p(y) - \mu_g^2 \sim \mathcal{O}(\epsilon^2) \quad (\text{B.11})$$

This implies,

$$\left(\frac{\sigma_g}{\mu_g}\right)^2 \sim \mathcal{O}\left(\frac{\epsilon^2}{g(y_a)^2}\right) \rightarrow \text{very small} \quad (\text{B.12})$$

Since we are looking at a minimum bound for N , we can safely neglect these small additive terms. Therefore, we are left with,

$$\left(\frac{\sigma_{fg}}{\mu_f \mu_g}\right)^2 \approx \left(\frac{\sigma_f}{\mu_f}\right)^2 \quad (\text{B.13})$$

It is not as simple to estimate the magnitude or place a bound on this quantity because, unlike the previous case, we do not have any further simplifying assumptions. In general, it can be shown that,

$$\left(\frac{\sigma_f}{\mu_f}\right)^2 \leq \frac{(x_b - x_a)^2}{4x_a x_b} \xrightarrow{x_b \gg x_a} \mathcal{O}(1/r_g) \quad (\text{B.14})$$

Where, as in the main text, $r_g = g_{a\gamma\gamma}^L / g_{a\gamma\gamma}^M \equiv x_a / x_b$. Since r_g is always less than unity, this provides a bound on N that is finite, but not necessarily small. However, this bound represents an extreme case based on the discrete two point distribution (where the probabilities are concentrated on the endpoints of the interval only) and, while true, does not provide a good description for the continuous and nice distributions that we are interested in. Unfortunately, in order to place a better bound, one needs to make certain assumptions on the kind of distribution functions we have (which would be model dependent) - this can improve the above result significantly. However, since such a treatment depends on the kind of models we have, we instead simply highlight that for simple uniform distributions, we have,

$$\left(\frac{\sigma_f}{\mu_f}\right)^2 = \frac{(x_b - x_a)^2}{3(x_b + x_a)^2} \xrightarrow{x_b \gg x_a} \frac{1}{3} \Rightarrow N > \frac{1}{3\epsilon} \quad (\text{B.15})$$

For $\epsilon = 0.1$, we find that the condition holds true for $N > 4$; this suggests that values of $N \sim \mathcal{O}(10)$ should be sufficient for our results to broadly hold in practice. As noted earlier, it does not seem possible to formulate a more general bound applicable for all distributions without some further simplifying assumptions; nevertheless, for physically relevant distributions, it is reasonable to expect that $N \sim \mathcal{O}(10)$ constitutes an adequate and reliable condition.

C Solution of the multi-ALP echo system

C.1 General solution

We start with,

$$(\partial_t^2 + p^2)\vec{A}_1^p = -2iN\vec{D}_{kp}e^{-ipt}Q(t) \quad (C.1)$$

And,

$$Q(t) = \int_{m_a^L}^{m_a^M} m_a \cos(m_a t) p(m_a) dm_a \quad (C.2)$$

In order to proceed further, we assume that the mass splitting, defined as $\epsilon = (m_a^M - m_a^L)/2$, is small. Then,

$$Q(t) = \int_{m_a^L}^{m_a^L + 2\epsilon} m_a \cos(m_a t) p(m_a) dm_a = \int_{m_a^L}^{m_a^L + 2\epsilon} h(m_a) dm_a = \bar{Q}(\epsilon, t) \quad (C.3)$$

Using the Leibniz rule,

$$\frac{d}{d\epsilon}\bar{Q}(\epsilon, t) = 2h(m_a^L + 2\epsilon), \quad \frac{d^2}{d\epsilon^2}\bar{Q}(\epsilon, t) = 4\frac{dh(m_a^L + 2\epsilon)}{d(m_a^L + 2\epsilon)}, \quad \frac{d^3}{d\epsilon^3}\bar{Q}(\epsilon, t) = 8\frac{d^2h(m_a^L + 2\epsilon)}{d(m_a^L + 2\epsilon)^2} \quad (C.4)$$

Taylor expanding, we have,

$$\begin{aligned} Q(t) \Big|_{m_a^M = m_a^L + 2\epsilon} &= \bar{Q}(0, t) + \epsilon \frac{d}{d\epsilon}\bar{Q}(0, t) + \frac{\epsilon^2}{2} \frac{d^2}{d\epsilon^2}\bar{Q}(0, t) + \frac{\epsilon^3}{6} \frac{d^3}{d\epsilon^3}\bar{Q}(0, t) + \dots \\ &= 2h(m_a^L)\epsilon + 2h'(m_a^L)\epsilon^2 + \frac{4}{3}h''(m_a^L)\epsilon^3 + \dots \end{aligned} \quad (C.5)$$

Now, we have,

$$h(m_a^L) = m_a^L \cos(m_a^L t) p(m_a^L), \quad (C.6a)$$

$$h'(m_a^L) = \cos(m_a^L t) p(m_a^L) - m_a^L t \sin(m_a^L t) p(m_a^L) + m_a^L \cos(m_a^L t) p'(m_a^L) \quad (C.6b)$$

Further,

$$\begin{aligned} h''(m_a^L) &= (-2t \sin(m_a^L t) - m_a^L t^2 \cos(m_a^L t)) p(m_a^L) \\ &\quad + (2 \cos(m_a^L t) - 2m_a^L t \sin(m_a^L t)) p'(m_a^L) + m_a^L \cos(m_a^L t) p''(m_a^L) \end{aligned} \quad (C.6c)$$

Or, to second order,

$$\begin{aligned} Q(t) \Big|_{m_a^M = m_a^L + 2\epsilon} &= 2m_a^L \cos(m_a^L t) p(m_a^L) \left[1 + \epsilon \left(\frac{1}{m_a^L} + \frac{p'(m_a^L)}{p(m_a^L)} \right) + \frac{2\epsilon^2}{3} \left(\frac{2p'(m_a^L)}{m_a^L p(m_a^L)} + \frac{p''(m_a^L)}{p(m_a^L)} \right) \right] \epsilon \\ &\quad - 2m_a^L t \sin(m_a^L t) p(m_a^L) \left[1 + \frac{4\epsilon}{3} \left(\frac{1}{m_a^L} + \frac{p'(m_a^L)}{p(m_a^L)} \right) \right] \epsilon^2 \end{aligned} \quad (C.7)$$

Therefore,

$$\begin{aligned} (\partial_t^2 + p^2)\vec{A}_1^p &= -4iN\vec{D}_{kp}^L f(\epsilon) e^{-ipt} \left[\cos(m_a^L t) \left[1 + \frac{\epsilon}{m_a^L} + \epsilon \frac{p'(m_a^L)}{p(m_a^L)} + \frac{2}{3}\epsilon^2 \left(\frac{2p'(m_a^L)}{m_a^L p(m_a^L)} + \frac{p''(m_a^L)}{p(m_a^L)} \right) \right] \right. \\ &\quad \left. - t \sin(m_a^L t) \left[1 + \frac{4\epsilon}{3} \left(\frac{1}{m_a^L} + \frac{p'(m_a^L)}{p(m_a^L)} \right) \right] \epsilon - \frac{2}{3}\epsilon^2 t^2 \cos(m_a^L t) \right] \end{aligned} \quad (C.8)$$

Here, $f(\epsilon) = p(m_a^L)\epsilon$. Let us write this as,

$$(\partial_t^2 + p^2)\vec{A}_1^p = -4iN\vec{D}_{kp}^L f(\epsilon)e^{-ipt} \left[a_1 \cos(m_a^L t) - a_2 \sin(m_a^L t)\epsilon t - \frac{2}{3}\epsilon^2 t^2 \cos(m_a^L t) \right] \quad (\text{C.9})$$

Here,

$$a_1 = \left[1 + \epsilon \left(\frac{1}{m_a^L} + \frac{p'(m_a^L)}{p(m_a^L)} \right) + \epsilon^2 b \right], \quad b = \frac{2}{3} \left[\frac{p'(m_a^L)}{m_a^L p(m_a^L)} + \frac{p''(m_a^L)}{p(m_a^L)} \right], \quad (\text{C.10a})$$

$$a_2 = \left[1 + \frac{4\epsilon}{3} \left(\frac{1}{m_a^L} + \frac{p'(m_a^L)}{p(m_a^L)} \right) \right] \quad (\text{C.10b})$$

Also, $\vec{D}_{kp}^L = \vec{D}_{kp} m_a^L$. Now, we need the solution to this. As outlined in appendix A, our solution is given by,

$$\vec{u}_p = \frac{i}{2p} e^{-ipt} \int_0^t d\xi \vec{G}(\xi) e^{ip\xi} - \frac{i}{2p} e^{ipt} \int_0^t d\xi \vec{G}(\xi) e^{-ip\xi} \quad (\text{C.11})$$

Where,

$$\vec{G}(t) = -4iN\vec{D}_{kp}^L f(\epsilon)e^{-ipt} \left[a_1 \cos(m_a^L t) - a_2 \sin(m_a^L t)\epsilon t - \frac{2}{3}\epsilon^2 t^2 \cos(m_a^L t) \right] \quad (\text{C.12})$$

The first integral can be computed in a straightforward fashion,

$$\begin{aligned} \int_0^t d\xi \vec{G}(\xi) e^{ip\xi} &= -4iN\vec{D}_{kp}^L f(\epsilon) \int_0^t d\xi \left[a_1 \cos(m_a^L \xi) - a_2 \sin(m_a^L \xi)\epsilon \xi - \frac{2}{3}\epsilon^2 \xi^2 \cos(m_a^L \xi) \right] \\ &= -4iN\vec{D}_{kp}^L f(\epsilon) \left[\frac{a_1}{m_a^L} \sin(m_a^L t) + \frac{\epsilon a_2}{(m_a^L)^2} [m_a^L t \cos(m_a^L t) - \sin(m_a^L t)] \right. \\ &\quad \left. - \frac{2\epsilon^2}{3(m_a^L)^3} [2m_a^L t \cos(m_a^L t) + ((m_a^L t)^2 - 2) \sin(m_a^L t)] \right] \\ &\equiv -4iN\vec{D}_{kp}^L f(\epsilon) \mathcal{Q}_1(p, t) \end{aligned} \quad (\text{C.13})$$

Similarly, let us take a look at the second integral,

$$\int_0^t d\xi \vec{G}(\xi) e^{-ip\xi} = -4iN\vec{D}_{kp}^L f(\epsilon) \int_0^t d\xi \left[a_1 \cos(m_a^L \xi) - a_2 \sin(m_a^L \xi)\epsilon \xi - \frac{2}{3}\epsilon^2 \xi^2 \cos(m_a^L \xi) \right] e^{-2ip\xi} \quad (\text{C.14})$$

Let us define (for $\alpha \in \mathbb{R}$ and $\alpha \neq 0$),

$$\mathcal{J}_n^\pm(\alpha, t) = \int_0^t d\xi \xi^n e^{\pm i\alpha \xi} = \mp \frac{i}{\alpha} t^n e^{\pm i\alpha t} \pm \frac{i}{\alpha} n \int_0^t d\xi \xi^{n-1} e^{\pm i\alpha \xi} = \mp \frac{i}{\alpha} t^n e^{\pm i\alpha t} \pm \frac{i}{\alpha} n \mathcal{J}_{n-1}^\pm(\alpha, t) \quad (\text{C.15})$$

Here, $n \geq 0$. The base case is,

$$\mathcal{J}_0^\pm(\alpha, t) = \int_0^t d\xi e^{\pm i\alpha \xi} = \mp \frac{i}{\alpha} [e^{\pm i\alpha t} - 1] \quad (\text{C.16})$$

Then,

$$\mathcal{J}_1^\pm(\alpha, t) = \mp \frac{i}{\alpha} t e^{\pm i\alpha t} \pm \frac{i}{\alpha} \mathcal{J}_0^\pm(\alpha, t) = \mp \frac{i}{\alpha} t e^{\pm i\alpha t} \pm \frac{i}{\alpha} \left(\mp \frac{i}{\alpha} e^{\pm i\alpha t} \pm \frac{i}{\alpha} \right) = \mp \frac{i}{\alpha} t e^{\pm i\alpha t} + \frac{1}{\alpha^2} [e^{\pm i\alpha t} - 1] \quad (\text{C.17})$$

And,

$$\mathcal{J}_2^\pm(\alpha, t) = \mp \frac{i}{\alpha} t^2 e^{\pm i\alpha t} + \frac{2}{\alpha^2} t e^{\pm i\alpha t} \pm \frac{2i}{\alpha^3} [e^{\pm i\alpha t} - 1] \quad (\text{C.18})$$

Using these definitions, we can write,

$$\begin{aligned} \int_0^t d\xi \vec{G}(\xi) e^{-ip\xi} &= -4iN \vec{D}_{kp}^L f(\epsilon) \int_0^t d\xi \left[a_1 \cos(m_a^L \xi) - a_2 \sin(m_a^L \xi) \epsilon \xi - \frac{2}{3} \epsilon^2 \xi^2 \cos(m_a^L \xi) \right] e^{-2ip\xi} \\ &= -2iN \vec{D}_{kp}^L f(\epsilon) \left[a_1 \left[\mathcal{J}_0^+(m_a^L - 2p, t) + \mathcal{J}_0^-(m_a^L + 2p, t) \right] + ia_2 \epsilon \left[\mathcal{J}_1^+(m_a^L - 2p, t) \right. \right. \\ &\quad \left. \left. - \mathcal{J}_1^-(m_a^L + 2p, t) \right] - \frac{2}{3} \epsilon^2 \left[\mathcal{J}_2^+(m_a^L - 2p, t) + \mathcal{J}_2^-(m_a^L + 2p, t) \right] \right] \\ &\equiv -4iN \vec{D}_{kp}^L f(\epsilon) \mathcal{Q}_2(p, t) \end{aligned} \quad (\text{C.19})$$

Therefore, the total solution is,

$$\vec{A}_1^p = \frac{2}{p} N \vec{D}_{kp}^L f(\epsilon) [e^{-ipt} \mathcal{Q}_1(p, t) - e^{ipt} \mathcal{Q}_2(p, t)] \quad (\text{C.20})$$

With,

$$\begin{aligned} \mathcal{Q}_1(p, t) &= \frac{a_1}{m_a^L} \sin(m_a^L t) + \epsilon \frac{a_2}{(m_a^L)^2} [m_a^L t \cos(m_a^L t) - \sin(m_a^L t)] \\ &\quad - \frac{2\epsilon^2}{3(m_a^L)^3} [2m_a^L t \cos(m_a^L t) + ((m_a^L t)^2 - 2) \sin(m_a^L t)] \end{aligned} \quad (\text{C.21})$$

And,

$$\begin{aligned} \mathcal{Q}_2(p, t) &= \frac{1}{2} \left[a_1 \left[\mathcal{J}_0^+(m_a^L - 2p, t) + \mathcal{J}_0^-(m_a^L + 2p, t) \right] + ia_2 \epsilon \left[\mathcal{J}_1^+(m_a^L - 2p, t) - \mathcal{J}_1^-(m_a^L + 2p, t) \right] \right. \\ &\quad \left. - \frac{2}{3} \epsilon^2 \left[\mathcal{J}_2^+(m_a^L - 2p, t) + \mathcal{J}_2^-(m_a^L + 2p, t) \right] \right] \end{aligned} \quad (\text{C.22})$$

C.2 Resonant response

Let us consider the system at resonance, i.e., $p = m_a^L/2 + \delta$. It is quite clear the resonant term is $\mathcal{Q}_2(p, t)$ - specifically the terms with $(m_a^L - 2p)$ in their arguments. We consider only the dominant contributions,

$$\text{At resonance: } \mathcal{Q}_2(p, t) \approx \frac{1}{2} \left[a_1 \mathcal{J}_0^+(m_a^L - 2p, t) + i\epsilon a_2 \mathcal{J}_1^+(m_a^L - 2p, t) - \frac{2}{3} \epsilon^2 \mathcal{J}_2^+(m_a^L - 2p, t) \right] \quad (\text{C.23})$$

As per our earlier definitions, at resonance, the individual terms are,

$$\mathcal{J}_0^+(m_a^L - 2p, t) = i \frac{e^{-2i\delta t} - 1}{2\delta}, \quad \mathcal{J}_1^+(m_a^L - 2p, t) = it \frac{e^{-2i\delta t}}{2\delta} + \frac{e^{-2i\delta t} - 1}{4\delta^2} \quad (\text{C.24})$$

$$\mathcal{J}_2^+(m_a^L - 2p, t) = it^2 \frac{e^{-2i\delta t} - 1}{2\delta} + t \frac{e^{-2i\delta t}}{2\delta^2} - i \frac{e^{-2i\delta t} - 1}{4\delta^3} \quad (\text{C.25})$$

Therefore, at resonance,

$$\begin{aligned} \mathcal{Q}_2(p, t) &= \frac{1}{2} \left[i \frac{e^{-2i\delta t} - 1}{2\delta} \left(a_1 + \frac{\epsilon}{2\delta} a_2 + \frac{\epsilon^2}{3\delta^2} \right) - t e^{-2i\delta t} \left(\frac{\epsilon}{2\delta} a_2 + \frac{\epsilon^2}{3\delta^2} \right) - i \frac{\epsilon^2}{3\delta} t^2 e^{-2i\delta t} \right] \\ &= \frac{1}{2} \left[i \frac{e^{-2i\delta t} - 1}{2\delta} \left[1 + \frac{\epsilon}{m_a^L} + \epsilon \frac{p'(m_a^L)}{p(m_a^L)} + \epsilon^2 b + \frac{\epsilon}{2\delta} \left[1 + \frac{4\epsilon}{3} \left(\frac{1}{m_a^L} + \frac{p'(m_a^L)}{p(m_a^L)} \right) \right] + \frac{\epsilon^2}{3\delta^2} \right] \right. \\ &\quad \left. - \left[\left[1 + \frac{4\epsilon}{3} \left(\frac{1}{m_a^L} + \frac{p'(m_a^L)}{p(m_a^L)} \right) \right] \frac{\epsilon}{2\delta} + \frac{\epsilon^2}{3\delta^2} \right] t e^{-2i\delta t} - i \frac{\epsilon^2}{3\delta} t^2 e^{-2i\delta t} \right] \end{aligned} \quad (\text{C.26})$$

Let us expand the sums in orders of ϵ . We have,

$$\mathcal{O}(\epsilon^0) : i \frac{e^{-2i\delta t} - 1}{2\delta} = \sum_{n=1}^{\infty} \frac{(-t)^n}{n!} i^{n+1} (2\delta)^{n-1} \quad (\text{C.27})$$

And,

$$\begin{aligned} \mathcal{O}(\epsilon^1) : i \frac{e^{-2i\delta t} - 1}{2\delta} \left(\frac{1}{m_a^L} + \frac{1}{2\delta} + \frac{p'(m_a^L)}{p(m_a^L)} \right) - \frac{t}{2\delta} e^{-2i\delta t} \\ = \left[\frac{1}{m_a^L} + \frac{p'(m_a^L)}{p(m_a^L)} \right] \sum_{n=1}^{\infty} \frac{(-t)^n}{n!} i^{n+1} (2\delta)^{n-1} - \sum_{n=1}^{\infty} \frac{n}{(n+1)!} (-i)^n t^{n+1} (2\delta)^{n-1} \end{aligned} \quad (\text{C.28})$$

Finally,

$$\begin{aligned} \mathcal{O}(\epsilon^2) : \left[\frac{2}{3\delta} \left[\frac{1}{m_a^L} + \frac{p'(m_a^L)}{p(m_a^L)} \right] + \frac{1}{3\delta^2} \right] \left[i \frac{e^{-2i\delta t} - 1}{2\delta} - t e^{-2i\delta t} \right] + i b \frac{e^{-2i\delta t} - 1}{2\delta} - \frac{i}{3\delta} t^2 e^{-2i\delta t} \\ = b \sum_{n=1}^{\infty} \frac{(-t)^n}{n!} i^{n+1} (2\delta)^{n-1} - \frac{4}{3} \left[\frac{1}{m_a^L} + \frac{p'(m_a^L)}{p(m_a^L)} \right] \sum_{n=1}^{\infty} \frac{n}{(n+1)!} (-i)^n t^{n+1} (2\delta)^{n-1} \\ - \frac{1}{3} \sum_{n=1}^{\infty} \frac{n}{(n+2)n!} (-2)^n i^{n+1} t^{n+2} \delta^{n-1} \end{aligned} \quad (\text{C.29})$$

Putting everything together, we get,

$$\begin{aligned} \mathcal{Q}_2(p, t) &= \frac{1}{2} \sum_{n=1}^{\infty} \frac{(-it)^n}{n!} (2\delta)^{n-1} \left[i \left(1 + \frac{\epsilon}{m_a^L} + \epsilon \frac{p'(m_a^L)}{p(m_a^L)} + b \right) - \frac{n}{n+1} \left(1 + \frac{4\epsilon}{3m_a^L} + \epsilon \frac{4p'(m_a^L)}{3p(m_a^L)} \right) \epsilon t \right. \\ &\quad \left. - \frac{2in}{3(n+2)} \epsilon^2 t^2 \right] = \frac{1}{2} \sum_{n=1}^{\infty} \frac{(-it)^n}{n!} (2\delta)^{n-1} \left[i a_1 - \frac{n}{n+1} a_2 \epsilon t - \frac{2in}{3(n+2)} \epsilon^2 t^2 \right] \end{aligned} \quad (\text{C.30})$$

For $\delta \rightarrow 0$, we have,

$$\mathcal{Q}_2(p, t) = \frac{t}{2} \left[a_1 + \frac{i}{2} a_2 \epsilon t - \frac{2}{9} \epsilon^2 t^2 \right] \quad (\text{C.31})$$

C.3 Real space solution

Let us now consider the behaviour of our previous solution in the resonant limit,

$$\vec{A}_1^p = \frac{2}{p} N \vec{D}_{kp}^L f(\epsilon) [e^{-ipt} \mathcal{Q}_1(p, t) - e^{ipt} \mathcal{Q}_2(p, t)] \quad (\text{C.32})$$

Now, at each ϵ order, we can see that the terms of $\mathcal{Q}_2(p, t)$ are dominant since they are polynomials in t , as opposed to oscillatory terms. Thus,

$$\text{At resonance: } \vec{A}_1^p = -\frac{t}{p} N \vec{D}_{kp}^L f(\epsilon) e^{ipt} \left[a_1 + \frac{i}{2} a_2 \epsilon t - \frac{2}{9} \epsilon^2 t^2 \right] \quad (\text{C.33})$$

Thus, the solution in real space is,

$$\vec{A}(t, \vec{x}) = \vec{a}_0 e^{i(\vec{k} \cdot \vec{x} - kt)} - N \frac{\tilde{g} t}{2} (\hat{k} \times \vec{a}_0) \left[a_1 + \frac{i}{2} a_2 \epsilon t - \frac{2}{9} \epsilon^2 t^2 \right] e^{i(\vec{k} \cdot \vec{x} + kt)} \quad (\text{C.34})$$

Where,

$$\tilde{g} = m_a^L f(\epsilon) \mathcal{A}_0 \int_{g_{a\gamma\gamma}^L}^{g_{a\gamma\gamma}^M} g_{a\gamma\gamma} \tilde{p}(g_{a\gamma\gamma}) dg_{a\gamma\gamma} \quad (\text{C.35})$$

C.4 Power calculation

In order to estimate the power carried by the echo wave, we start from,

$$\mathcal{Q}_2(p, t) = \frac{1}{2} \sum_{n=1}^{\infty} \frac{(-it)^n}{n!} (2\delta)^{n-1} \left[ia_1 - \frac{n}{n+1} a_2 \epsilon t - \frac{2in}{3(n+2)} \epsilon^2 t^2 \right] \quad (\text{C.36})$$

We need to calculate the magnitude of the above to compute the power. Let us define,

$$\begin{aligned} \mathcal{Y}_1(x) &= -\frac{\epsilon t}{4\delta} \sum_{n=1}^{\infty} \frac{(-it)^n}{n!} (2\delta)^n \frac{x^n}{n+1} = -\frac{\epsilon t}{4\delta} \int_0^1 dy \sum_{n=1}^{\infty} \frac{(-it)^n}{n!} (2\delta)^n y^n x^n \\ &= -\frac{\epsilon t}{4\delta} \int_0^1 dy \left(e^{-2i\delta xy t} - 1 \right) \end{aligned} \quad (\text{C.37})$$

And,

$$\begin{aligned} \mathcal{Y}_2(x) &= -i \frac{\epsilon^2 t^2}{6\delta} \sum_{n=1}^{\infty} \frac{(-it)^n}{n!} (2\delta)^n \frac{x^n}{n+2} = -i \frac{\epsilon^2 t^2}{6\delta} \int_0^1 dy \sum_{n=1}^{\infty} \frac{(-2i\delta xt)^n}{n!} y^{n+1} \\ &= -i \frac{\epsilon^2 t^2}{6\delta} \int_0^1 dy y \left(e^{-2i\delta xy t} - 1 \right) \end{aligned} \quad (\text{C.38})$$

Then,

$$\mathcal{Q}_2(p, t) = a_1 \frac{i}{4\delta} (e^{-2i\delta t} - 1) + a_2 \frac{\partial \mathcal{Y}_1}{\partial x} \Big|_{x=1} + \frac{\partial \mathcal{Y}_2}{\partial x} \Big|_{x=1} = \frac{t}{2} \int_0^1 dy e^{-2i\delta y t} \left(a_1 + ia_2 \epsilon t y - \frac{2}{3} \epsilon^2 t^2 y^2 \right) \quad (\text{C.39})$$

The magnitude is,

$$\begin{aligned}
|\mathcal{Q}_2(p, t)|^2 &= \frac{t^2}{4} \int_0^1 dy \int_0^1 dx e^{2i\delta t(x-y)} \left[a_1 + ia_2\epsilon ty - \frac{2}{3}\epsilon^2 t^2 y^2 \right] \left[a_1 - ia_2\epsilon tx - \frac{2}{3}\epsilon^2 t^2 x^2 \right] \\
&= \frac{t^2}{4} \int_0^1 dy \int_0^1 dx e^{2i\delta t(x-y)} \left[a_1^2 + (a_2\epsilon t)^2 xy + ia_1 a_2 \epsilon t (y-x) - \frac{2}{3} a_1 \epsilon^2 t^2 (x^2 + y^2) \right. \\
&\quad \left. - \frac{2i}{3} a_2 \epsilon^3 t^3 xy (x-y) + \mathcal{O}(\epsilon^4) \right]
\end{aligned} \tag{C.40}$$

Clearly, if t is large, the exponential will oscillate rapidly - therefore, the major contribution will always be from the region where x, y are close to each other. Thus, let us define new variables,

$$\alpha = x + y, \quad \beta = x - y \tag{C.41}$$

The Jacobian is simply 1/2. Therefore,

$$\begin{aligned}
|\mathcal{Q}_2(p, t)|^2 &= \frac{t^2}{8} \int_{\mathcal{D}} d\alpha d\beta e^{2i\delta t\beta} \left[a_1^2 + ia_1 a_2 \epsilon t \beta + \left[\left(\frac{a_2^2}{4} - \frac{a_1}{3} \right) \alpha^2 - \left(\frac{a_2^2}{4} + \frac{a_1}{3} \right) \beta^2 \right] (\epsilon t)^2 \right. \\
&\quad \left. - \frac{i}{6} a_2 \epsilon^3 t^3 \beta (\alpha^2 - \beta^2) \right]
\end{aligned} \tag{C.42}$$

\mathcal{D} denotes the new region of integration after the change of variables,

$$\int_0^1 dx \int_0^1 dy \rightarrow \left(\int_0^1 \int_{-\alpha}^{\alpha} + \int_1^2 \int_{\alpha-2}^{2-\alpha} \right) d\beta d\alpha \tag{C.43}$$

Let us evaluate this integral term by term. We switch the β limits to cover the entire real line because the major contribution to the integral only comes from the small β region. We also ignore the fourth order term. We have,

$$\int_{-\infty}^{\infty} e^{2i\delta t\beta} d\beta = 2\pi\delta(2\delta t) = \frac{\pi}{t}\delta(\delta) \tag{C.44}$$

Further,

$$\int_{-\infty}^{\infty} \beta e^{2i\delta t\beta} d\beta \rightarrow 0 \text{ as } \delta \rightarrow 0 \tag{C.45}$$

The other odd term in β also vanishes similarly. Next,

$$\left(\int_0^1 \int_{-\alpha}^{\alpha} + \int_1^2 \int_{\alpha-2}^{2-\alpha} \right) \beta^2 e^{2i\delta t\beta} d\beta d\alpha \xrightarrow{\lim \delta \rightarrow 0} 2\pi\delta(2\delta t) \left(\int_0^1 \int_{-\alpha}^{\alpha} + \int_1^2 \int_{\alpha-2}^{2-\alpha} \right) \beta^2 d\beta d\alpha = \frac{\pi}{3t}\delta(\delta) \tag{C.46}$$

Putting everything together,

$$\begin{aligned}
|\mathcal{Q}_2(p, t)|^2 &= \frac{t^2}{8} \int_{\mathcal{D}} d\alpha d\beta e^{2i\delta t\beta} \left[a_1^2 + ia_1 a_2 \epsilon t \beta + \left[\left(\frac{a_2^2}{4} - \frac{a_1}{3} \right) \alpha^2 - \left(\frac{a_2^2}{4} + \frac{a_1}{3} \right) \beta^2 \right] (\epsilon t)^2 \right] \\
&= \frac{\pi t}{4} \delta(\delta) \left[a_1^2 + \frac{7}{24} \left(a_2^2 - \frac{12}{7} a_1 \right) \epsilon^2 t^2 \right]
\end{aligned} \tag{C.47}$$

Therefore, the power is,

$$\begin{aligned}
P_N^\epsilon &= \int dp |\tilde{A}_1^p|^2 = \int dp \frac{4N^2}{p^2} |\tilde{D}_{kp}^L f(\epsilon)|^2 |\mathcal{Q}_2(p, t)|^2 \\
&= \frac{4\pi t \mathcal{A}_0^2 N^2}{16} [m_a^L f(\epsilon)]^2 \left[\int_{g_{a\gamma\gamma}^L}^{g_{a\gamma\gamma}^M} g_{a\gamma\gamma} \tilde{p}(g_{a\gamma\gamma}) dg_{a\gamma\gamma} \right]^2 \left[a_1^2 + \frac{7}{24} \left(a_2^2 - \frac{12}{7} a_1 \right) \epsilon^2 t^2 \right] \frac{dP_0}{dp} \Big|_{p=m_a^L/2}
\end{aligned} \tag{C.48}$$

Now, the DM density is given by,

$$\rho = \frac{1}{2} \sum_{n=1}^N (m_a^n)^2 \mathcal{A}_0^2 = \frac{1}{2} N \mathcal{A}_0^2 \int_{m_a^L}^{m_a^L+2\epsilon} m_a^2 p(m_a) dm_a \equiv \frac{1}{2} N \mathcal{A}_0^2 I(\epsilon) \tag{C.49}$$

Where,

$$I(\epsilon) = \int_{m_a^L}^{m_a^L+2\epsilon} m_a^2 p(m_a) dm_a = \int_{m_a^L}^{m_a^L+2\epsilon} h(m_a) dm_a \tag{C.50}$$

Taylor expanding and proceeding as before, we have,

$$\begin{aligned}
I(\epsilon) &= 2(m_a^L)^2 p(m_a^L) \epsilon \left[1 + \epsilon \left(\frac{1}{m_a^L} + \frac{p'(m_a^L)}{p(m_a^L)} \right) + \frac{2\epsilon^2}{3} \left(\frac{2p'(m_a^L)}{m_a^L p(m_a^L)} + \frac{p''(m_a^L)}{p(m_a^L)} \right) \right] \\
&\quad + 2m_a^L p(m_a^L) \left[1 + \frac{4\epsilon}{3} \left(\frac{1}{m_a^L} + \frac{p'(m_a^L)}{p(m_a^L)} \right) \right] \epsilon^2 + \dots
\end{aligned} \tag{C.51}$$

Thus,

$$\rho = N \mathcal{A}_0^2 (m_a^L)^2 f(\epsilon) \left[a_1 + \frac{\epsilon}{m_a^L} a_2 \right] \tag{C.52}$$

Therefore, our final expression for the power is,

$$P_N^\epsilon = 2N \mathcal{Z}(\epsilon, t) P_{N=1} \Big|_{g_{a\gamma\gamma}^M} \tag{C.53}$$

Where,

$$\mathcal{Z}(\epsilon, t) = f(\epsilon) \left[\int_{g_{a\gamma\gamma}^L}^{g_{a\gamma\gamma}^M} \frac{g_{a\gamma\gamma}}{g_{a\gamma\gamma}^M} \tilde{p}(g_{a\gamma\gamma}) dg_{a\gamma\gamma} \right]^2 \left[a_1 + \frac{\epsilon}{m_a^L} a_2 \right]^{-1} \left[a_1^2 + \frac{7}{24} \left(a_2^2 - \frac{12}{7} a_1 \right) \epsilon^2 t^2 \right] \tag{C.54}$$

Here, $P_{N=1}$ refers to the power in the original, single ALP case.

Acknowledgments

SH would like to thank Jayanta K. Bhattacharjee, Anuraj Chatterjee and Tanmoy Kumar for several helpful discussions. SH would also like to acknowledge the KVPY fellowship provided by the Department of Science and Technology (DST), Government of India.

References

- [1] R.D. Peccei and H.R. Quinn, CP conservation in the presence of pseudoparticles, *Phys. Rev. Lett.* **38** (1977) .
- [2] S. Weinberg, A new light boson?, *Phys. Rev. Lett.* **40** (1978) 223.
- [3] F. Wilczek, Problem of strong p and t invariance in the presence of instantons, *Phys. Rev. Lett.* **40** (1978) 279.
- [4] A.P. Zhitnitskii, Possible suppression of axion-hadron interactions, *Sov. J. Nucl. Phys. (Engl. Transl.); (United States)* **31** (1980) .
- [5] M. Dine, W. Fischler and M. Srednicki, A simple solution to the strong cp problem with a harmless axion, *Phys. Lett. B* **104** (1981) 199.
- [6] J.E. Kim, Weak-interaction singlet and strong CP invariance, *Phys. Rev. Lett.* **43** (1979) 103.
- [7] M.A. Shifman, A. Vainshtein and V. Zakharov, Can confinement ensure natural cp invariance of strong interactions?, *Nucl. Phys. B* **166** (1980) 493.
- [8] L.F. Abbott and P. Sikivie, A cosmological bound on the invisible axion, *Phys. Lett. B* **120** (1983) 133.
- [9] J. Preskill, M.B. Wise and F. Wilczek, Cosmology of the invisible axion, *Phys. Lett. B* **120** (1983) 127.
- [10] M. Dine and W. Fischler, The not so harmless axion, *Phys. Lett. B* **120** (1983) 137.
- [11] G. Alonso-Álvarez, J.M. Cline and T. Xiao, The flavor of QCD axion dark matter, *J. High Energ. Phys.* **07** (2023) 187.
- [12] M. Bauer, M. Neubert and A. Thamm, Collider probes of axion-like particles, *J. High Energ. Phys.* **44** (2017) .
- [13] K. Mimasu and V. Sanz, Alps at colliders, *J. High Energ. Phys.* **2015** (2015) .
- [14] A. Caputo and G. Raffelt, Astrophysical axion bounds: The 2024 edition, *PoS COSMICWISPers* (2024) 041.
- [15] C.A.J. O’Hare, Cosmology of axion dark matter, *PoS COSMICWISPers* (2024) 040.
- [16] D.J.E. Marsh, Axion Cosmology, *Phys. Rept.* **643** (2016) 1 [1510.07633].
- [17] P. Sikivie, Axion Cosmology, *Lect. Notes Phys.* **741** (2008) 19 [astro-ph/0610440].
- [18] G. Raffelt and L. Stodolsky, Mixing of the photon with low-mass particles, *Phys. Rev. D* **37** (1988) 1237.
- [19] A. Arza, Photon enhancement in a homogeneous axion dark matter background, *Eur. Phys. J. C* **79** (2019) 250.
- [20] A. Arza and P. Sikivie, Production and detection of an axion dark matter echo, *Phys. Rev. Lett.* **123** (2019) 131804.
- [21] A. Arza and E. Todarello, Axion dark matter echo: A detailed analysis, *Phys. Rev. D* **105** (2022) 023023.
- [22] A. Arza, A. Kryemadhi and K. Zioutas, Searching for axion streams with the echo method, *Phys. Rev. D* **108** (2023) 083001.

- [23] A. Arza, Q. Guo, L. Wu, Q. Yang, X. Yang, Q. Yuan et al., *Listening for echo from the stimulated axion decay with the 21 centimeter array*, *Sci. Bull.* **69** (2024) 2971.
- [24] A. Caputo, M. Regis, M. Taoso and S.J. Witte, *Detecting the Stimulated Decay of Axions at Radio Frequencies*, *J. Cosmo. Astropart. Phys.* **03** (2019) 027.
- [25] M.A. Buen-Abad, J. Fan and C. Sun, *Axion echoes from the supernova graveyard*, *Phys. Rev. D* **105** (2022) 075006.
- [26] Y. Sun, K. Schutz, A. Nambrath, C. Leung and K. Masui, *Axion dark matter-induced echo of supernova remnants*, *Phys. Rev. D* **105** (2022) 063007.
- [27] O. Ghosh, J. Salvado and J. Miralda-Escudé, *Axion gegenschein: Probing back-scattering of astrophysical radio sources induced by dark matter*, *arXiv:2008.02729 [astro-ph.CO]* (2020) .
- [28] A. Caputo, C.P.n. Garay and S.J. Witte, *Looking for Axion Dark Matter in Dwarf Spheroidals*, *Phys. Rev. D* **98** (2018) 083024.
- [29] E. Todarello, F. Calore and M. Regis, *Anatomy of astrophysical echoes from axion dark matter*, *J. Cosmo. Astropart. Phys.* **05** (2024) 040.
- [30] A. Arvanitaki, S. Dimopoulos, S. Dubovsky, N. Kaloper and J. March-Russell, *String axiverse*, *Phys. Rev. D* **81** (2010) 123530.
- [31] P. Svrcek and E. Witten, *Axions in string theory*, *J. High Energ. Phys.* **06** (2006) 051.
- [32] I. Broeckel, M. Cicoli, A. Maharana, K. Singh and K. Sinha, *Moduli stabilisation and the statistics of axion physics in the landscape*, *J. High Energ. Phys.* **08** (2021) 059.
- [33] D.E. Kaplan and R. Rattazzi, *Large field excursions and approximate discrete symmetries from a clockwork axion*, *Phys. Rev. D* **93** (2016) 085007.
- [34] K. Choi and S.H. Im, *Realizing the relation from multiple axions and its uv completion with high scale supersymmetry*, *J. High Energ. Phys.* **01** (2016) 149.
- [35] G.F. Giudice and M. McCullough, *A clockwork theory*, *J. High Energ. Phys.* **02** (2017) 036.
- [36] S. Bhattacharya, D. Choudhury, S. Maharana and T. Srivastava, *Axion icebergs: Clockwork alps at hadron colliders*, *arXiv:2409.05983 [hep-ph]* (2024) .
- [37] F. Chadha-Day, J. Maxwell and J. Turner, *Alp anarchy*, *J. Cosmo. Astropart. Phys.* **2024** (2024) 056.
- [38] CAST collaboration, *New CAST Limit on the Axion-Photon Interaction*, *Nature Phys.* **13** (2017) 584.
- [39] D. Kondo and H. Murayama, *Multiple Axions Save High-Scale Inflation*, *arXiv:2507.07973 [hep-ph]* (2025) .
- [40] D.I. Dunskey, C.A. Manzari, P. Quilez, M. Ramos and P. Sørensen, *Resonant Landau-Zener Conversion In Multi-Axion Systems*, *arXiv:2507.06287 [hep-ph]* (2025) .
- [41] M.S. Turner, *Cosmic and Local Mass Density of Invisible Axions*, *Phys. Rev. D* **33** (1986) 889.
- [42] L.D. Duffy and P. Sikivie, *The Caustic Ring Model of the Milky Way Halo*, *Phys. Rev. D* **78** (2008) 063508 [0805.4556].
- [43] S.S. Chakrabarty, Y. Han, A.H. Gonzalez and P. Sikivie, *Implications of triangular features in the Gaia skymap for the Caustic Ring Model of the Milky Way halo*, *Phys. Dark Univ.* **33** (2021) 100838 [2007.10509].

- [44] M. Bastero-Gil, C. Beaufort and D. Santos, *Solar axions in large extra dimensions*, [*J. Cosmo. Astropart. Phys.* **10** \(2021\) 048](#).
- [45] ADMX collaboration, *SQUID-Based Microwave Cavity Search for Dark-Matter Axions*, [*Phys. Rev. Lett.* **104** \(2010\) 041301](#).
- [46] ADMX collaboration, *A Search for Invisible Axion Dark Matter with the Axion Dark Matter Experiment*, [*Phys. Rev. Lett.* **120** \(2018\) 151301](#).
- [47] ADMX collaboration, *Extended Search for the Invisible Axion with the Axion Dark Matter Experiment*, [*Phys. Rev. Lett.* **124** \(2020\) 101303](#).
- [48] ADMX collaboration, *Search for Invisible Axion Dark Matter in the 3.3–4.2 μeV Mass Range*, [*Phys. Rev. Lett.* **127** \(2021\) 261803](#).
- [49] ADMX collaboration, *Piezoelectrically Tuned Multimode Cavity Search for Axion Dark Matter*, [*Phys. Rev. Lett.* **121** \(2018\) 261302](#).
- [50] ADMX collaboration, *Dark matter axion search using a Josephson Traveling wave parametric amplifier*, [*Rev. Sci. Instrum.* **94** \(2023\) 044703](#).
- [51] N. Crisosto, P. Sikivie, N.S. Sullivan, D.B. Tanner, J. Yang and G. Rybka, *ADMX SLIC: Results from a Superconducting LC Circuit Investigating Cold Axions*, [*Phys. Rev. Lett.* **124** \(2020\) 241101](#).
- [52] J. Jeong, S. Youn, S. Bae, J. Kim, T. Seong, J.E. Kim et al., *Search for Invisible Axion Dark Matter with a Multiple-Cell Haloscope*, [*Phys. Rev. Lett.* **125** \(2020\) 221302](#).
- [53] Y. Lee, B. Yang, H. Yoon, M. Ahn, H. Park, B. Min et al., *Searching for Invisible Axion Dark Matter with an 18 T Magnet Haloscope*, [*Phys. Rev. Lett.* **128** \(2022\) 241805](#).
- [54] CAPP collaboration, *First Results from an Axion Haloscope at CAPP around 10.7 μeV* , [*Phys. Rev. Lett.* **126** \(2021\) 191802](#).
- [55] H. Yoon, M. Ahn, B. Yang, Y. Lee, D. Kim, H. Park et al., *Axion haloscope using an 18 T high temperature superconducting magnet*, [*Phys. Rev. D* **106** \(2022\) 092007](#).
- [56] J.O. Burns et al., *Nasa probe study report: Farside array for radio science investigations of the dark ages and exoplanets (farside)*, [*arXiv:1911.08649 \[astro-ph.IM\]* \(2019\)](#).
- [57] J.O. Burns et al., *A lunar farside low radio frequency array for dark ages 21-cm cosmology*, [*arXiv:2103.08623 \[astro-ph.IM\]* \(2021\)](#).
- [58] X. Chen, J. Yan, L. Deng, F. Wu, L. Wu, Y. Xu et al., *Discovering the sky at the longest wavelengths with a lunar orbit array*, [*Phil. Trans. R. Soc. A* **379** \(2021\)](#).
- [59] A. Taruya, A. Nishizawa and Y. Himemoto, *Hunting axion dark matter signatures in low-frequency terrestrial magnetic fields*, [*arXiv:2504.06653 \[hep-ph\]* \(2025\)](#).
- [60] A. Nishizawa, A. Taruya and Y. Himemoto, *Axion dark matter search from terrestrial magnetic fields at extremely low frequencies*, [*arXiv:2504.07559 \[hep-ph\]* \(2025\)](#).
- [61] J.N. Benabou, C. Dessert, K.C. Patra, T.G. Brink, W. Zheng, A.V. Filippenko et al., *Search for axions in magnetic white dwarf polarization at lick and keck observatories*, [*arXiv:2504.12377 \[hep-ph\]* \(2025\)](#).
- [62] S.M. Ross, *Introduction to Probability Models*, Elsevier, 12th ed. (2014), [10.1016/C2012-0-03564-8](#).